Article

Not peer-reviewed version

The Reduction of Rotating Conveyor Roller Vibrations by the Use of Plastic Brackets

Leopold Hrabovský * , Eliška Nováková , Štěpán Pravda , Daniel Kurač , Tomáš Machálek

Posted Date: 22 November 2023

doi: 10.20944/preprints202311.1342.v1

Keywords: laboratory machine; plastic holder; conveyor roller; conveyor idler; vibration; measurement of vibration velocities

Article

The Reduction of Rotating Conveyor Roller Vibrations by the Use of Plastic Brackets

Leopold Hrabovský *, Eliška Nováková, Štěpán Pravda, Daniel Kurač and Tomáš Machálek

Department of Machine and Industrial Design, Faculty of Mechanical Engineering, VSB-Technical University of Ostrava, 708 00 Ostrava, Czech Republic; eliska.novakova.fs1@vsb.cz (E.N), stepan.pravda@vsb.cz (S.P.), daniel.kurac.st@vsb.cz (D.K), tomas.machalek@vsb.cz (T.M).

* Correspondence: leopold.hrabovsky@vsb.cz (L.H.)

Abstract: The paper presents the basic structural parts, a 3D model and the overall design of a laboratory machine, which was created to detect vibrations generated by the casing of a conveyor roller rotating at different speeds. The intention of the authors was to verify whether plastic brackets inserted into the structurally modified trestles of a fixed conveyor idler can reduce the vibration values transmitted from the rotating conveyor roller to the trestle of a fixed idler. Experimental vibration measurements taken on the non-rotating parts of conveyor rollers, performed on a laboratory machine according to ISO 10816, are suitable for characterizing their operating conditions with regard to trouble-free operation. The aim of this paper is to detect the vibrations of a rotating conveyor roller on a laboratory machine in the defined places of a fixed conveyor idler and also on the steel frame of a laboratory machine that represents the supporting track of a belt conveyor. Vibrations detected by piezoelectric acceleration sensors were recorded by a measuring apparatus and displayed in the environment of Dewesoft X software. The measurements show that the vibration values grow with the increasing speed of the conveyor roller rotation. Experimental measurements have proven the correctness of the assumption that the vibrations transmitted to the trestle of a fixed conveyor idler are lower by up to 40% when using plastic brackets into which the axle of the conveyor roller is attached, compared to the solution where the axle of the conveyor roller is inserted into the notches of a steel trestle.

Keywords: laboratory machine; plastic holder; conveyor roller; conveyor idler; vibration; measurement of vibration velocities

1. Introduction

Vibration [1,2] is defined as a process during which a material body oscillates around its equilibrium position. Vibration [3] is described by amplitude and phase at a given point in time. Since in real situations, a body cannot be described as a single point of mass, the oscillation through the body spreads gradually from one particle to another—this phenomenon is called waves. Waves can be classified as non-periodic and periodic. Periodic waves [4] (harmonic vibrations) have a sinusoidal waveform and can be described by their speed, acceleration and deflection. These three quantities are the basis for the description and measurement of vibrations [5]. We use speed mainly to determine the energy of vibrations, acceleration to determine the high-frequency components of vibrations, and deflection is used for low-frequency components.

The CSN ISO 10816 standard [6] establishes the general rules for measuring and evaluating machine vibrations, and these vibrations are measured on non-rotating parts (especially on bearings). The standard [6] stipulates that the measurement is generally broadband in order to cover the entire frequency range of a particular machine being measured. According to the standard [6], the measured values are the vibration deflection, vibration velocity and vibration acceleration. In practice, the effective value of vibration velocity is mainly used for vibration evaluation due to its relationship with the energy of these vibrations. Two criteria are decisive for the assessment of vibration strength (the highest measured value from a set of vibrations performed at multiple locations and in multiple directions). The first is the magnitude of the vibration, and the second is the magnitude of the change in vibration [7].

Preprints (www.preprints.org) | NOT PEER-REVIEWED | Posted: 22 November 2023 doi:10.20944/preprints202311.1342.v1

By vibrations [8] we mean the mechanical oscillation of a body or elastic medium, where the individual points of the body/medium oscillate around an equilibrium position. The motion of the individual points of a body subjected to vibrations can be described by the time course of its deflection y(t) [m], velocity v(t) [m·s^{-1}] [9] or acceleration a(t) [m·s^{-2}] (1).

$$a(t)=\frac{d^2y(t)}{dt^2}=\frac{d^2A\cdot\sin(\omega t)}{dt^2}=\frac{dv(t)}{dt}=\frac{dA\cdot\omega\cos(\omega t)}{dt^2}=-A\cdot\omega^2\cdot\sin(\omega t)\,[ms^{-2}], \quad (1)$$

The effective value of vibration acceleration a_{RMS} [m·s^{-2}] can be expressed as (2).

$$a_{RMS}=\sqrt{\frac{1}{T}\cdot\int_0^T\left|a^2(t)\right|\cdot dt}=\frac{|a_{max}|}{\sqrt{2}}\approx 0.707\cdot A\cdot\omega^2\,[ms^{-2}], \quad (2)$$

In the article [10], by the authors Perun and Opasiak, vibration measurements of the cylinder shell installed on a laboratory stand were made. It contains the results of the assessment of the technical condition of the rollers of belt conveyors after a specified period of operation.

Klimenda et al. [11] deals with the measurement of noise and vibration of rollers for belt conveyors. In this article is described and individual rollers types which were measured. Process of noise and vibration measurement of the individual rollers types is given. Part of the article is noise and vibration measurement evaluation. Three the highest acceleration values in depending on the frequency of vibration in individual directions (*x*, *y*, *z*) are given.

In the article [12] Svoboda et al. deal with measuring vibrations on the stand of a roller conveyor. Difference between individual set of rollers is in used of semi-finished product of the outer shell, the design of the rollers is the same. One set has a shell from convectional tube and the second set from accuracy tube. The vibrations were measured by six-channel analyser Brüel & Kjær (PULSE). Acceleration and natural frequency were measured by using a three-axis accelerometer. In the conclusion of the article is an evaluation of vibration. Three the highest acceleration values in depending on the frequency of vibration in individual directions are given. From this evaluation are selected rollers with minimal and maximal acceleration.

In the article [13] Bortnowski et al. created a device for a wireless measuring device that moves with the conveyor belt along of the route, which records the signal of transverse vibrations of the belt.

The roller is an important part of the belt conveyor in sand carrier at sea, presented by Peng et al in the article [14]. They in this paper, a novel intelligent fault diagnosis method for rollers is proposed by using audio wavelet packet decomposition and Convolutional Neural Networks (CNN).

Article by M. Svoboda et al. [15] deals with the measurement of vibrations on the stand of a roller conveyor. Acceleration and natural frequency were measured by using a three-axis accelerometer. In the conclusion of the article is an evaluation of vibration. Three the highest acceleration values in depending on the frequency of vibration in individual directions are given.

In many branches of industry, bulk materials are transported over short, medium and long transport distances using continuously working conveyor systems, the so-called belt conveyors [16–18]. The conveyor belt, see Figure 1, consists of a conveyor line 1 (assembled from steel assembled parts), which is fitted with conveyor rollers 2 [19] that support the conveyor belt 3 [20]. The endless loop of the conveyor belt circulates between two end drums. As a rule, on the upper surface of the conveyor belt, guided in the upper run of the belt conveyor [21], the conveyed material is transported towards the driving station.

Preprints (www.preprints.org) | NOT PEER-REVIEWED | Posted: 22 November 2023 doi:10.20944/preprints202311.1342.v1

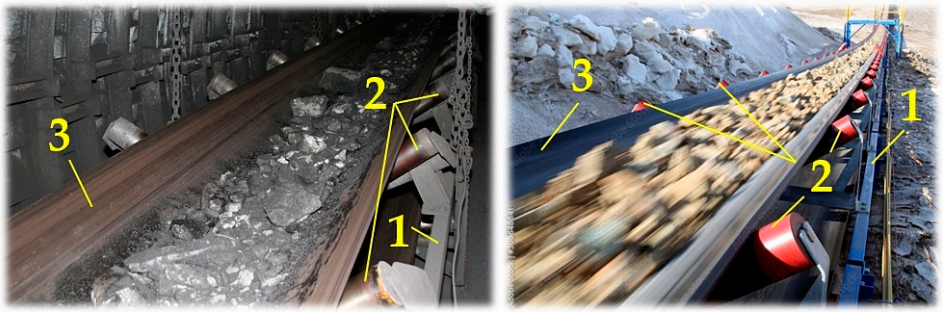

Figure 1. The endless loop of a conveyor belt supported by conveyor rollers.

On the drive drum of a conveyor belt driving station, the conveyor belt is carried away by frictional forces acting on the contact surface between the surface of the drive drum casing and the surface of the conveyor belt. The solution of the force ratios acting on the driving drums is based on the basic Euler (Eytelwein) relation [22,23]. The transmission capability [24,25] between the drive drum and the conveyor belt depends on the angle of wrap, the coefficient of friction between the belt and the drive drum, and the belt tension (which generates the tension force of the conveyor belt).

Belt conveyor drives must be designed in such a way that the belt on the driving drums does not slip in the individual movement phases (start-up, steady running, and run-down phases). It is possible to increase the transmission capacity of belt conveyor drives by a number of technical measures, including e. g. increasing the coefficient of friction between the belt and the drive drum, increasing the preload of the conveyor belt and increasing the angle of wrap (the implementation of two-drum and three-drum driving stations).

The disadvantage of both two-drum (Figure 2ab) and three-drum drives is that the working run of the conveyor belt touches the casings of the conveyor rollers in the return run of the belt conveyor. An insufficiently cleaned surface of a conveyor belt from the adhered grains of the transported material causes the material to stick to the casings of the conveyor rollers, see Figure 2c. These then vibrate as a result of the unbalanced mass when the rollers rotate.

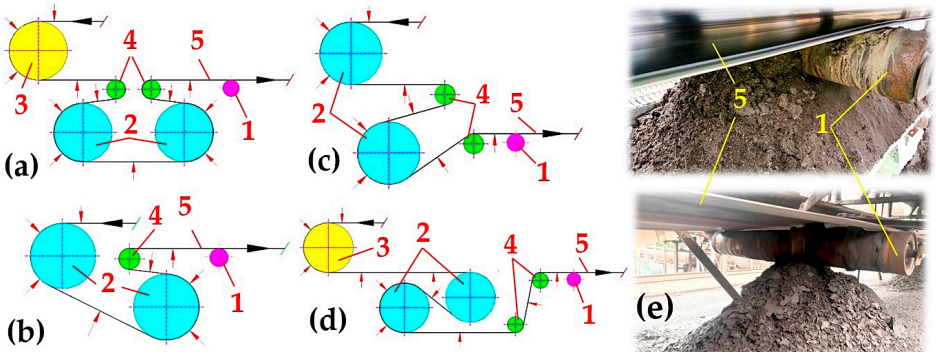

Figure 2. Two-drum driving station **(a)** type Ω, **(b)** type C, **(c)** without a boom, **(d)** type S, **(e)** transported material stuck on the casing of the conveyor roller. 1—conveyor roller, 2—drive drum, 3—dump drum, 4—transmission drum, 5—conveyor belt.

In Figure 2a to Figure 2d, the red arrows indicate the working surface of the conveyor belt, i.e. the surface on which the conveyed material is carried in the working (upper) run of the conveyor belt. In the return run of the conveyor belt, this dirty surface of the conveyor belt meets the casings of the conveyor rollers [26]. Despite the intensive brushing of dirt and adhered material grains from the working surface of the conveyor belt with devices called cleaners [27–30], dirt often remains on the surfaces of the conveyor belts, which accumulates on the rotating casings of the conveyor rollers.

Authors J Eliasson et al. in article [31] they present an Internet of Things (IoT) architecture suitable for large scale sensor networks for condition monitoring. The developed technology has been applied and demonstrated for rotating conveyor belt rolls.

Preprints (www.preprints.org) | NOT PEER-REVIEWED | Posted: 22 November 2023 doi:10.20944/preprints202311.1342.v1

Authors R. Li et al. propose in the article [32] to use radial grating vibration sensing technology for both belt conveyor roller vibration monitoring. This can then be used to predict the fault state in the roller and its position, using distributed optical fibber temperature measurement technology which can be used for "hot spot monitoring".

This paper [33] presents a recent review of acoustic and vibration signal-based fault detection for belt conveyor idlers using ML models. It also discusses major steps in the approaches, such as data collection, signal processing, feature extraction and selection, and ML model construction.

Article [34] by X Liu et al. describes a test device for detecting vibration of conveyor belt rollers.

Machine learning-based techniques for condition monitoring and fault diagnosis of industrial equipment were used in the paper [35] by authors J. Soares et al. Therefore, this paper presents a machine learning-based method for fault diagnosis in belt conveyor idlers.

2. Materials and Methods

The article is a follow-up to the article [9], in which the effective values of the vibration velocity v_{RMS} [m·s^{-1}] were measured in three mutually perpendicular planes of a rotating (circumferential speed v_r = 1.28 to 6.93 m·s^{-1}) conveyor roller (with the casing diameter of 133 mm). The effective values of the vibration velocity v_{RMS} [m·s^{-1}] were measured for two different fittings of the conveyor roller axles. One is the traditional placement of the flattened ends of the roller axle in the notches of the trestles, see Figure 3b on the fixed conveyor idler. The second way is to position these flattened ends of the roller axle in plastic brackets inserted into the specially designed steel trestles of the fixed conveyor idler.

The measurement of the effective values of vibration velocity v_{RMS} [m·s^{-1}] was done using a laboratory machine, see Figure 3a, which is located in a laboratory at the Department of Machine and Industrial Design, Faculty of Mechanical Engineering, VSB-Technical University of Ostrava. This device was designed by DvB-AF s.r.o., with its registered office at Meleček 227, 747 41 Hradec nad Moravicí, Žimrovice. A laboratory stand designed to measure the noise of a rotating roller is described in [36,37].

Researches on idlers were rather focused on rolling resistance, their energy consumption, load distribution, and failure analysis until now [38–41].

A 3D structural model of a laboratory machine created in SolidWorks®Premium 2012x64, SP5 is shown in Figure 3. The laboratory machine consists of a steel frame 1, to which a vertically sliding drive support frame is mechanically attached 7, see Figure 3c. The supporting device of the electric motor 8 is attached to the supporting frame of the drive 7, to which the electric motor is attached by screw connections (type 1AL90L-4, power engine P_e = 1.5 kW, revolutions n_e = 1445 min^{-1}). A V-belt pulley with a calculated diameter of d_w = 81.5 mm, is positioned onto the shaft of an electric ϕ 24 mm (with a tight key 8 x 7 x 40 mm). This pulley transmits the pulling force of the drive by friction to one (or two) V-belts 5 [42] (type SPZ 2500 Lw 9.7 x 2513 La L=L). The revolutions of the electric motor n_e [min^{-1}] is controlled by an electric inverter (type YASKAWA VS-606 V7).

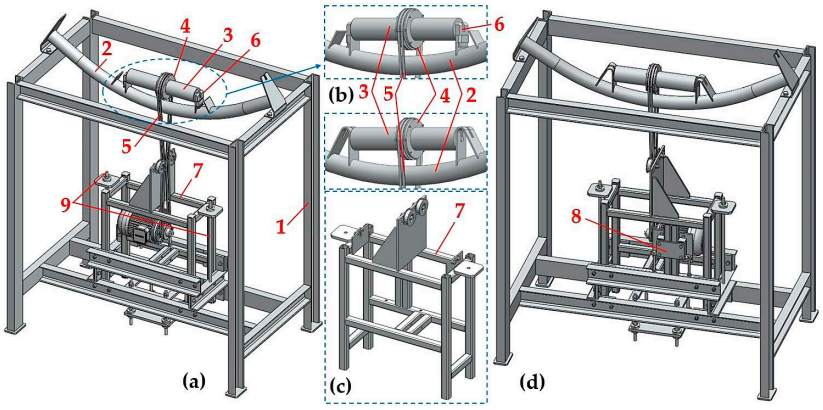

Figure 3. (a) Structural 3D design of a laboratory machine—front view, **(b)** conveyor roller placed in the trestle of a fixed conveyor idler, **(c)** drive frame, **(d)** laboratory machine—rear view. 1—steel

Preprints (www.preprints.org) | NOT PEER-REVIEWED | Posted: 22 November 2023 doi:10.20944/preprints202311.1342.v1

frame, 2—fixed conveyor idler, 3—conveyor roller, 4—driven pulley, 5—V-belt, 6—plastic bracket, 7—drive support frame, 8—electric motor support device.

Laboratory measurements were carried out on conveyor rollers with various diameters D_r [mm] (133, 108 and 89), at the same circumferential speeds v_r [m·s^{-1}] of their casings.

In Table 1, it is possible to read the required circumferential speed v_r [m·s^{-1}] of the conveyor roller, the required revolutions n_r [min^{-1}] of a roller with diameter D_r [m] and frequency f_i [Hz], by which the revolutions n_r [min^{-1}] of a conveyor roller is controlled by a frequency converter.

Table 1. Calculated values of the rotational speed n_r [min^{-1}] of a conveyor roller with a given diameter D_r [m] for circumferential speed v_r [m·s^{-1}] of the conveyor roller casings.

D_r [mm]		89			108			133			
f_i [Hz]	v_r [m·s^{-1}]	n_r [s^{-1}]	n_r [min^{-1}]	f_i [Hz]	v_r [m·s^{-1}]	n_r [s^{-1}]	n_r [min^{-1}]	f_i [Hz]	v_r [m·s^{-1}]	n_r [s^{-1}]	n_r [min^{-1}]
50	3.58	12.81	768.7	50	4.35	12.82	769.2	50	5.35	12.80	768.3
34.9	2.5	8.94	536.5	41.2	3.58	10.55	633.1	33.4	3.58	10.41	624.7
17.4	1.25	4.47	268.2	28.8	2.5	7.37	442.1	23.4	2.5	5.98	359.0
-	-	-	-	14.4	1.25	3.68	221.0	11.7	1.25	2.99	179.5

The theoretical magnitude of rotational speed n_r [m·s^{-1}] of the conveyor roller with diameter D_r [m] can be expressed based on knowing the transmission ratio i_w [-] and the constant c_i [-] according to the relation (3). The transmission ratio i_w [-] is defined by the ratio of the calculated diameter of the drive pulley d_w [m] and the diameter of the driven pulley D_w [m]. The constant c_i [-] expresses the ratio of the frequency value of f = 50 Hz (in Europe a unified distribution grid of 400/230V with a frequency of 50 Hz is used. In North America, it is a phase distribution system of 120V at a frequency of 60 Hz) and the frequency f_i [Hz] set on the display of the frequency converter.

$$n_r = n_e \cdot i_w \cdot c_i = n_e \cdot \frac{d_W}{D_W} \cdot \frac{f}{f_i} \; [s^{-1}], \tag{3}$$

One or two so-called "V-belt pulley assembly" units are placed onto the tested conveyor roller (with a steel, plastic or rubberized casing) with a diameter of D_r = 133 mm (or 108 mm or 89 mm), see Figure 4a. This assembly consists of a flange 2, with screw connections 3 attaching a pulley 1 with the calculated diameter of D_w = 153 mm. Prevention of this flange displacement 2 along the length of the conveyor roller casing, and prevention of flange rotation in relation to the circumference of the conveyor roller casing, is secured via screw connections 4.

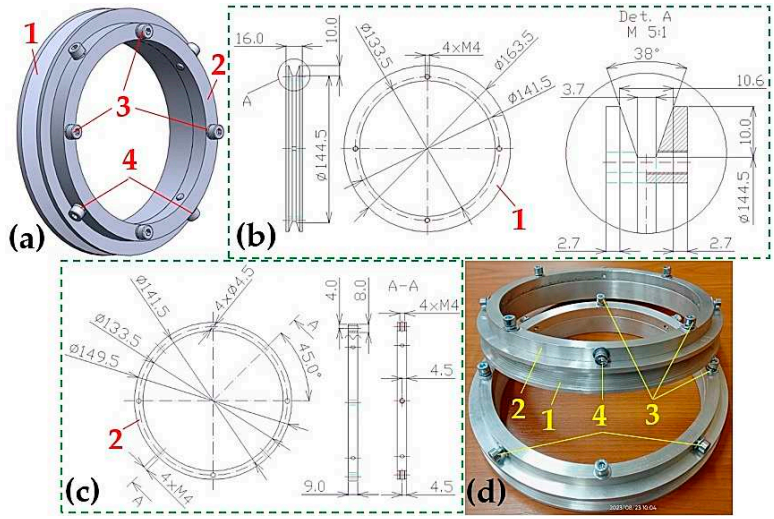

Figure 4. (a) A 3D model of V-belt pulley assembly, **(b)** the dimensions of the pulley, **(c)** the dimensions of the flange for the conveyor roller ϕ133 mm, **(d)** manufactured V-belt pulley assembly. 1—V-belt pulley, 2—flange, 3—screw M4x16 DIN 912, 4—screw M4x10 DIN 912.

Preprints (www.preprints.org) | NOT PEER-REVIEWED | Posted: 22 November 2023 doi:10.20944/preprints202311.1342.v1

An electric motor [43], on the shaft of which a V-belt is slid (calculated diameter d_w = 81.5 mm), sets the V-belt into motion [42]. The V-belt rotates the test conveyor roller at a revolution n_r [min^{-1}], corresponding to the circumferential velocity v_r [$m \cdot s^{-1}$] of the conveyor roller, see Table 1.

The design dimensions of flange 2 slid onto the ϕ108 mm conveyor roller is shown in Figure 5b, and the design dimensions of flange 2 slid onto the ϕ89 mm conveyor roller is shown in Figure 5e.

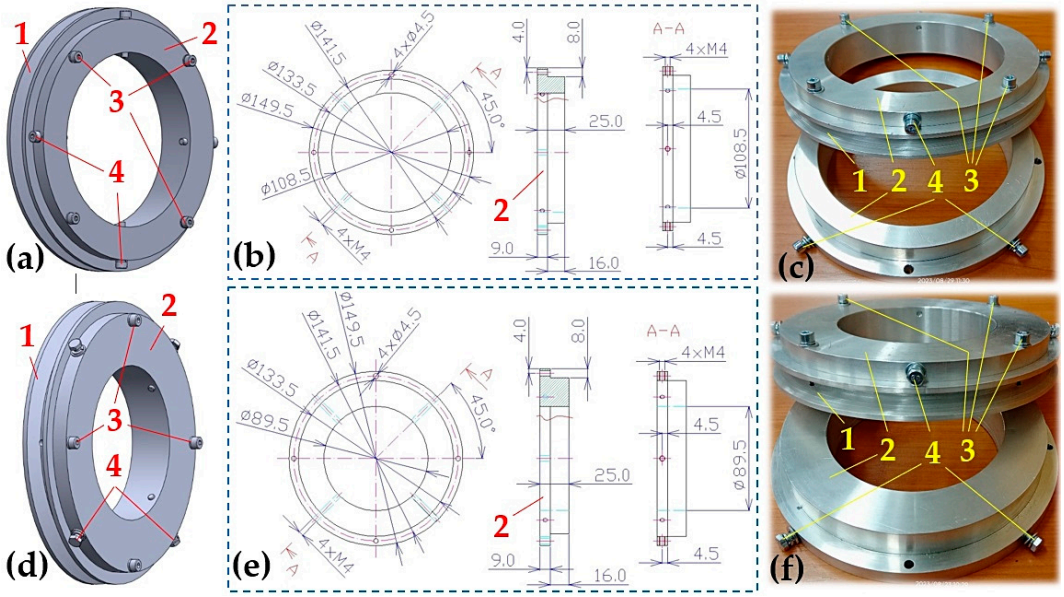

Figure 5. (a) A 3D model of the V-belt pulley assembly, **(b)** flange dimensions for ϕ108 mm conveyor roller, **(c)** manufacture V-belt pulley assembly, **(d)** a 3D model of the V-belt pulley assembly, **(e)** flange dimensions for ϕ89 mm conveyor roller, **(f)** manufactured V-belt pulley assembly. 1—V-belt pulley, 2—flange, 3—screw M4x16 DIN 912, 4—screw M4x25 DIN 912 (screw M4x35 DIN 933).

Steel casing, see Figure 6a, or rubberized, see Figure 6b, conveyor roller (ϕ133, ϕ108 or ϕ89 mm) rotates relative to the stable axle of the roller ϕ20 mm on 2 pcs of radial ball bearings 6204-2RS [44].

In the article [45] the authors M. Vasić et al. analysed failures of belt conveyor tension roller bearings. The article also examines the effects of tensioner pulley mounting position on bearing damage.

Figure 6. Conveyor roller **(a)** steel, **(b)** rubberized, **(c)** a 3D model of a conveyor roller fitted with two pieces V-belt pulley assembly. 1—V-belt pulley, 2—flange, 3—screw M4x16 DIN 912, 4—screw M4x10 (25) DIN 912 (M4x35 DIN 933), 5—conveyor roller ϕ133 mm (or ϕ108 mm or ϕ89 mm).

Plastic casing, see Figure 7a, of the conveyor roller (ϕ133, ϕ108 or ϕ89 mm) rotates relative to the roller axle ϕ20 mm on 2 radial ball bearings 6204-2RS [44].

Preprints (www.preprints.org) | NOT PEER-REVIEWED | Posted: 22 November 2023 doi:10.20944/preprints202311.1342.v1

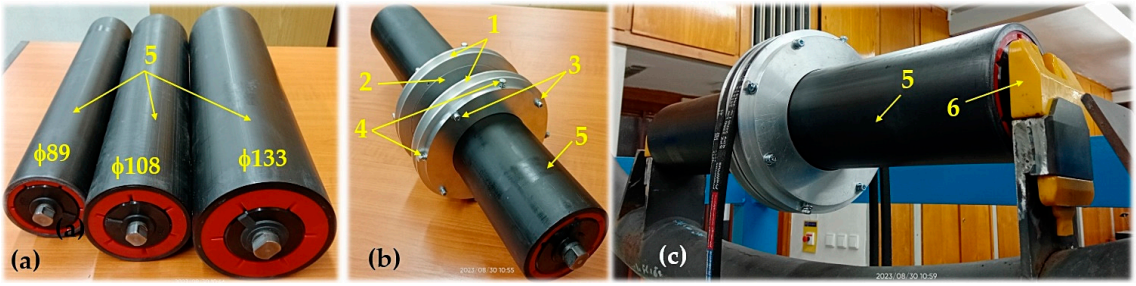

Figure 7. (a) plastic conveyor roller, **(b)** conveyor roller fitted with two pieces of a V-belt pulley assembly, **(c)** roller axle placed in a plastic bracket. 1—V-belt pulley, 2—flange, 3—screw M4x16 DIN 912, 4—screw M4x10 (25) DIN 912 (M4x35 DIN 933), 5—conveyor roller ϕ133 mm (or ϕ108 mm, or ϕ89 mm), 6—plastic bracket to hold the roller axles.

The axle of the tested conveyor roller is inserted into a cut-out in the steel (Figure 3b) or plastic (Figure 8d) trestle of the fixed conveyor idler, which is screwed to the top surface of the steel frame of the laboratory machine (Figure 3).

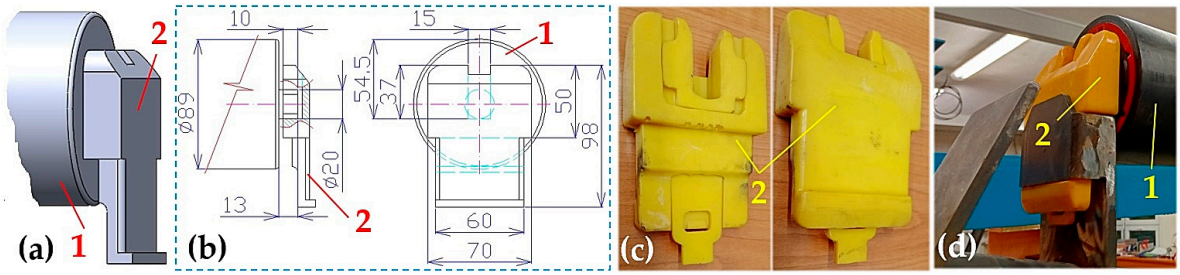

Figure 8. Plastic bracket for the conveyor roller axle inserted into a modified trestle of a fixed roller idler **(a)** 3D structural design, **(b)** 3D structural design, **(c)** the implemented solution of the plastic bracket, plastic holder, **(d)** conveyor roller mounted in the trestle of a fixed roller idler. 1—conveyor roller, 2—plastic bracket.

The vibrations generated by the rotating conveyor roller, transmitted to the sleeper of the fixed roller idler and the steel frame of the laboratory machine, were detected by two acceleration sensors PCE KS903.10 [46], see Figure 9. Signals from acceleration sensors were recorded by Dewesoft SIRIUSi-HS 6xACC, 2xACC+ [47] measuring apparatus during experimental measurements. Time records of the measured vibration values were used by the Dewesoft X [48] measuring program and transformed into effective vibration velocity values $v_{(*)RMS(fi)}$ [mm·s^{-1}] in the range of 10÷1·10^4 Hz (this frequency range is applied in the ISO 10816-3 standard [49]). Effective velocity values $v_{(*)RMS(fi)}$ [mm·s^{-1}] (where * presents the x, y or z axis of the coordinate system) with periodic courses were displayed using a PS monitor in the environment of the Dewesoft X measuring software.

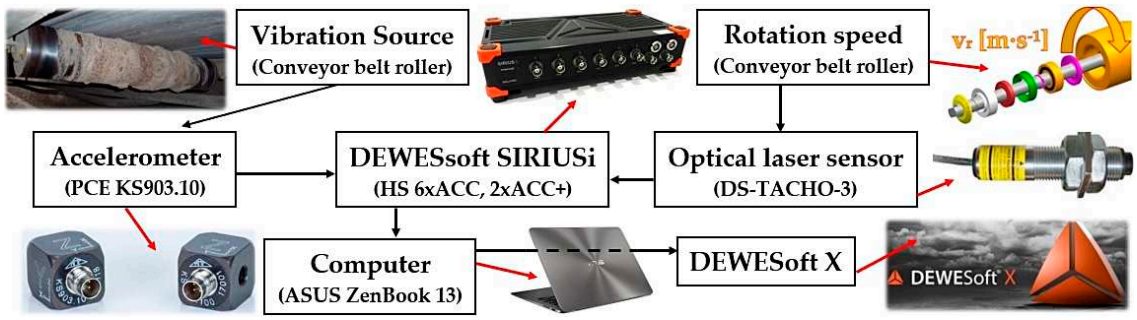

Figure 9. Measuring chain for detecting and recording the vibrations of rotating rollers on a laboratory machine.

The speed of the conveyor roller was scanned by an optical laser sensor DS-TACHO-3 [50,51].

Preprints (www.preprints.org) | NOT PEER-REVIEWED | Posted: 22 November 2023 doi:10.20944/preprints202311.1342.v1

3. Results

The aim of this paper is to specify an academic contribution, which is one of the possible recommendations to reduce the vibrations transmitted to the supporting structure of the belt conveyor excited by the rotating casing of the conveyor roller.

Experimental measurements of vibration velocities $v_{(*)RMS(fi)}$ [mm·s^{-1}] for a rotating conveyor roller with a diameter D_r [mm] were done using a laboratory machine, see Figure 3, under the same technical conditions, on two types of fixed conveyor idlers (where basic dimensions comply with the standard CSN ISO 1537 [52]), see Figure 10a. The fixed roller idler support consists of rollers with diameter D_r [mm], with their axles firmly embodied in the cut-outs of trestles 1, placed on a sleeper 2 made of a tube with a circular cross-section.

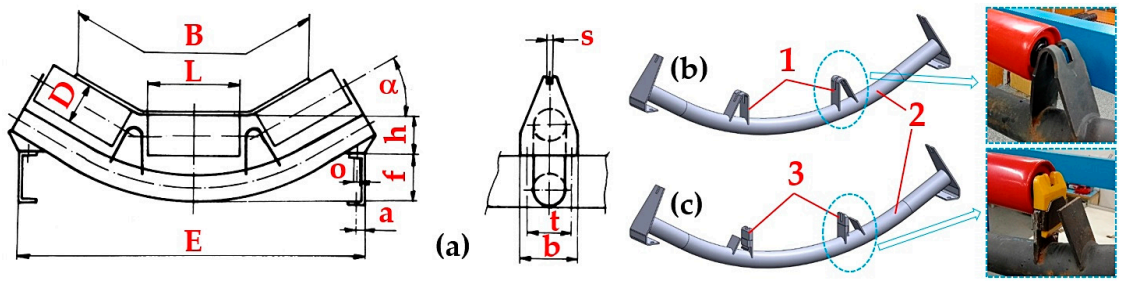

Figure 10. (a) fixed conveyor idler—basic dimensions (in Table 2), **(b)** roller support with traditional trestles, **(c)** conveyor idler with plastic brackets in trestles. 1—trestle, 2—sleeper, 3—plastic bracket.

Interventionary studies involving animals or humans, and other studies that require ethical approval, must list the authority that provided approval and the corresponding ethical approval code.

Table 2. Basic dimensions of the conveyor idler according to [52].

E	D = D_r	L	a	b	t	o	s	h	f	α	weight
		[mm]								[deg]	[kg]
1200	1600	89, 108, 133	465	35	140	100	18	14	85	175	20	18.5

The experimental measurement of vibration velocities $v_{(*)RMS(fi)}$ [mm·s^{-1}] was carried out in a central roller (horizontally placed roller in a fixed idler), see Figure 10a, of our laboratory machine. A conveyor roller of a given diameter D_r [mm] fitted with a V-belt pulley assembly, see Figures 4a and 5a,d, was rotated by means of a V-belt [42] with revolutions n_r [min^{-1}] (see Table 1). Using two acceleration sensors [46] the vibrations of the rotating conveyor roller positioned in the trestle were detected (B or D), see Figure 11, in the fixed conveyor idler and at the point of the mechanical attachment of the roller support to the upper beam of the steel frame of the laboratory machine (A or C), see Figure 11.

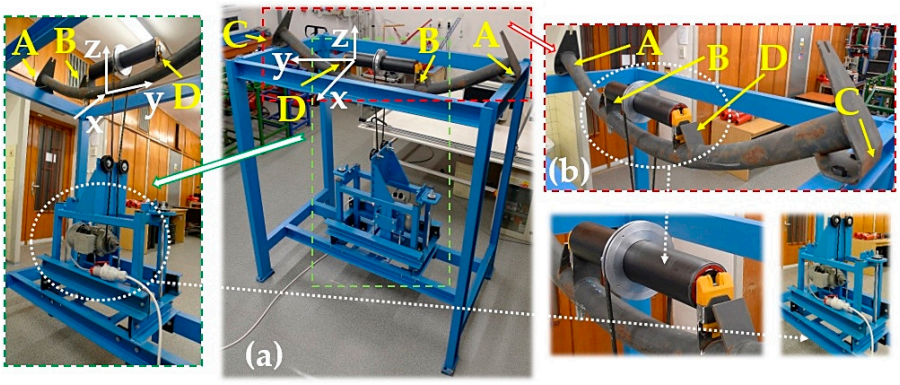

Figure 11. (a) A laboratory machine used to measure the vibrations of the conveyor rollers; (b) measuring points A, B, C, and D on a fixed conveyor idler where accelerometers are placed.

Preprints (www.preprints.org) | NOT PEER-REVIEWED | Posted: 22 November 2023 doi:10.20944/preprints202311.1342.v1

3.1. The plastic Trestle of a Fixed Conveyor idler, the Plastic Casing of the Conveyor Roller

Table 3 indicates effective vibration velocity values $v_{(*)RMS(fi)}$ [mm·s^{-1}], which have been read from the DEWESoft X measurement software, for the vibration measurements of a conveyor roller with a diameter of 89 mm plastic casing at the measuring points A and B for a fixed conveyor idler with plastic brackets (Figure 8) of our laboratory machine (Figure 11).

Table 3. Roller axle placement—plastic trestle, measuring points A and B, roller casing—plastic, D_r = 89 mm.

f_i	n_r	v_r	Measuring point „A“			Measuring point „B“		
			V(x)RMS(fi)	V(y)RMS(fi)	V(z)RMS(fi)	V(x)RMS(fi)	V(y)RMS(fi)	V(z)RMS(fi)
[Hz]	[min^{-1}]	[m·s^{-1}]		[mm·s^{-1}]			[mm·s^{-1}]	
50	825	3.84	0.93 [1]	0.31 [1]	0.21 [1]	0.47 [2]	0.17 [2]	0.92 [2]
32.5	536	2.50	0.23	0.21	0.10	0.52	0.14	0.62
16.2	268	1.25	0.14	0.10	0.07	0.14	0.08	0.22

[1] see Figure 12a, [2] see Figure 12b.

Figure 12 indicates the measured effective values of the vibration speed $v_{(*)RMS(50)}$ [mm·s^{-1}] in the "x", "y" and "z" axes of the selected coordinate system at circumferential speed v_r = 3.84 m·s^{-1} for a conveyor roller with a plastic casing of 89 mm diameter.

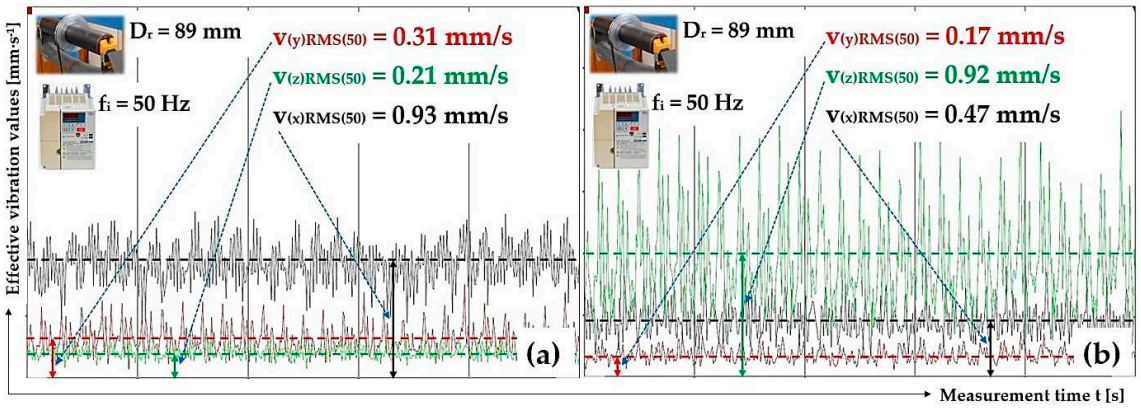

Figure 12. Effective vibration values $v_{(*)RMS(fi)}$ [mm·s^{-1}], plastic roller ϕ89 mm, the circumferential speed of the roller v_r = 3.84 m·s^{-1}, plastic trestle, **(a)** measuring point A, **(b)** measuring point B.

With regard to the scope of the paper, the measured graphs of the effective values of vibration velocities $v_{(*)RMS(fi)}$ [mm·s^{-1}] are not presented in this paper for circumferential speeds v_r = 2.5 m·s^{-1} and v_r = 1.25 m·s^{-1} for conveyor rollers with a diameter of 89 mm. In case of interest in these measured vibration waveforms, the author of this paper can supply the measured data sets with the graphic records of the measured vibration values for the conveyor rollers (with a steel or plastic casing), whose axles are placed in plastic brackets, Figure 10c, or on a steel trestle, Figure 10b, of the fixed conveyor idler.

Table 4 indicates effective vibration velocity values $v_{(*)RMS(fi)}$ [mm·s^{-1}], which have been read from the DEWESoft X measurement software, for the vibration measurements of a conveyor roller with a diameter of 89 mm plastic casing at the measuring points C and D for a fixed conveyor idler with plastic brackets.

Preprints (www.preprints.org) | NOT PEER-REVIEWED | Posted: 22 November 2023 doi:10.20944/preprints202311.1342.v1

Table 4. Roller axle placement—plastic trestle, measuring points C and D, roller casing—plastic, D_r = 89 mm.

f_i	n_r	v_r	Measuring point „C“			Measuring point „D“		
			$V_{(x)RMS(fi)}$	$V_{(y)RMS(fi)}$	$V_{(z)RMS(fi)}$	$V_{(x)RMS(fi)}$	$V_{(y)RMS(fi)}$	$V_{(z)RMS(fi)}$
[Hz]	[min^{-1}]	[m·s^{-1}]		[mm·s^{-1}]			[mm·s^{-1}]	
50	825	3.84	0.87 [1]	0.25 [1]	0.13 [1]	0.40 [2]	0.14 [2]	0.93 [2]
32.4	535	2.49	1.61	0.20	0.12	1.03	0.12	0.65
16.2	267	1.25	0.12	0.12	0.08	0.26	0.06	0.23

[1] see Figure 13a, [2] see Figure 13b.

Figure 13 shows the measured effective values of the vibration speed $v_{(*)RMS(50)}$ [mm·s^{-1}] in three mutually perpendicular axes of the coordinate system (Figure 11) at circumferential speed v_r = 3.84 m·s^{-1} of the conveyor roller with a plastic casing diameter 89 mm. Vibration sensors have been placed at measuring points C and D.

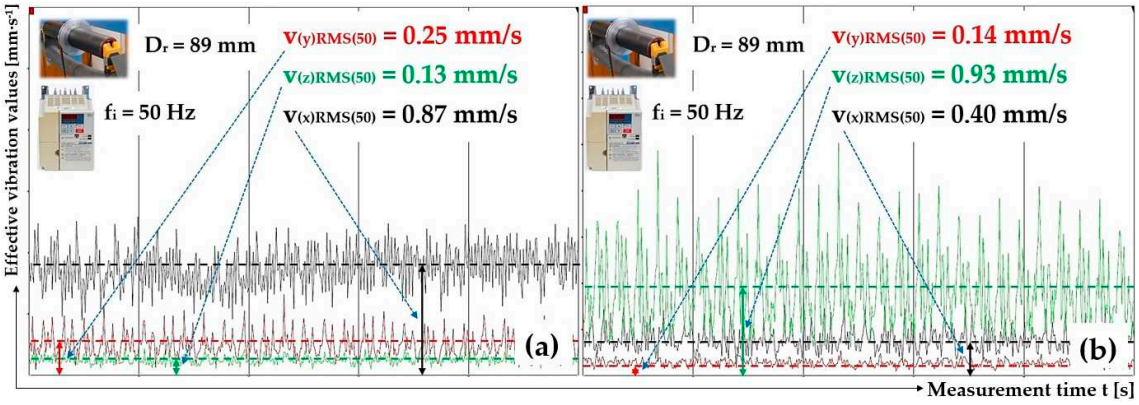

Figure 13. Effective vibration values $v_{(*)RMS(fi)}$ [mm·s^{-1}], plastic roller ϕ89 mm, the circumferential speed of the roller v_r = 3.84 m·s^{-1}, plastic trestle, **(a)** measuring point C, **(b)** measuring point D.

Table 5 indicates effective vibration velocity values $v_{(*)RMS(fi)}$ [mm·s^{-1}], which have been read from the DEWESoft X measurement software, for the vibration measurements of a conveyor roller with a diameter of 89 mm plastic casing at the measuring points C and D for a fixed conveyor idler with plastic brackets.

Table 5. Roller axle placement—plastic trestle, measuring points A and B, roller casing—plastic, D_r = 108 mm.

f_i	n_r	v_r	Measuring point “A”			Measuring point “B”		
			$V_{(x)RMS(fi)}$	$V_{(y)RMS(fi)}$	$V_{(z)RMS(fi)}$	$V_{(x)RMS(fi)}$	$V_{(y)RMS(fi)}$	$V_{(z)RMS(fi)}$
[Hz]	[min^{-1}]	[m·s^{-1}]			[mm·s^{-1}]			
50	824	4.66	0.92	0.26	0.25	0.46	0.22	0.70
41.3	681	3.85	0.88	0.36	0.22	0.53	0.29	1.03
26.8	442	2.5	0.60 [1]	0.14 [1]	0.13 [1]	0.25 [2]	0.10 [2]	0.34 [2]
13.4	220	1.24	0.09	0.08	0.06	0.08	0.05	0.17

[1] see Figure 14a, [2] see Figure 14b.

Figure 14 shows the measured effective values of the vibration speed $v_{(*)RMS(50)}$ [mm·s^{-1}] in three mutually perpendicular axes of the coordinate system (Figure 11) at circumferential speed v_r = 2.5 m·s^{-1} of the conveyor roller with a plastic casing diameter 108 mm. Vibration sensors have been placed at measuring points A and B.

Preprints (www.preprints.org) | NOT PEER-REVIEWED | Posted: 22 November 2023 doi:10.20944/preprints202311.1342.v1

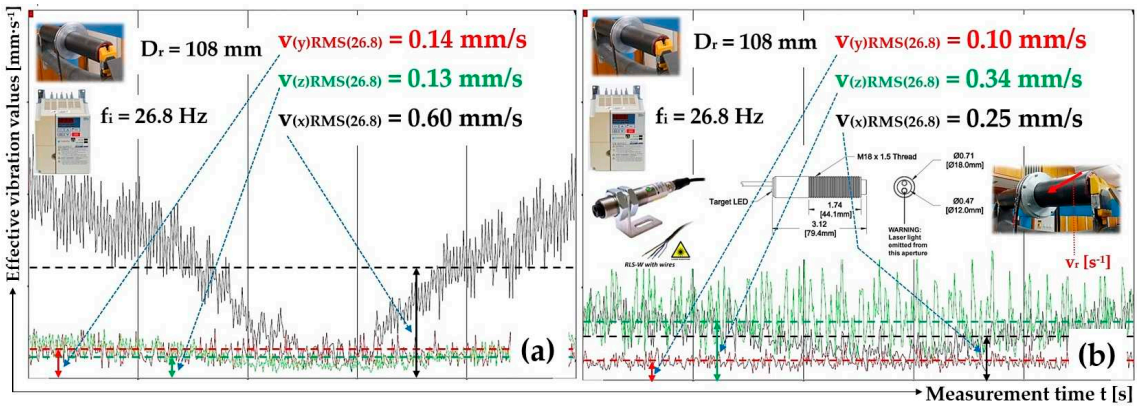

Figure 14. Effective vibration values $v_{(*)RMS(fi)}$ [mm·s^{-1}], plastic roller ϕ108 mm, the circumferential speed of the roller v_r = 2.5 m·s^{-1}, plastic trestle, **(a)** measuring point A, **(b)** measuring point B.

In this paper, the measured graphs of the effective values of vibration velocities $v_{(*)RMS(fi)}$ [mm·s^{-1}] are not presented for the circumferential speeds of the conveyor rollers (with diameter 108 mm and 133 mm.) other than v_r = 2.5 m·s^{-1}. As mentioned above, if you are interested in these measured vibration waveforms, it is necessary to ask the authors of this article via e-mail for documentation of the measured vibration records of the conveyer rollers taken at various circumferential speeds v_r [m·s^{-1}].

Table 6. Roller axle placement—plastic trestle, measuring points C and D, roller casing—plastic, D_r = 108 mm.

f_i	n_r	v_r	Measuring point „C"			Measuring point „D		
			V(x)RMS(fi)	V(y)RMS(fi)	V(z)RMS(fi)	V(x)RMS(fi)	V(y)RMS(fi)	V(z)RMS(fi)
[Hz]	[min^{-1}]	[m·s^{-1}]	[mm·s^{-1}]					
50	824	4.66	0.55	0.23	0.11	0.36	0.21	0.72
41.3	681	3.85	0.52	0.33	0.09	0.41	0.26	0.96
26.8	442	2.5	0.56 [1]	0.12 [1]	0.07 [1]	0.21 [2]	0.09 [2]	0.34 [2]
13.4	220	1.24	0.11	0.06	0.06	0.09	0.10	0.15

[1] see Figure 15a, [2] see Figure 15b.

Figure 15 indicates the measured effective values of the vibration speed $v_{(*)RMS(50)}$ [mm·s^{-1}] in the "x", "y" and "z" axes of the selected coordinate system at circumferential speed v_r = 2.5 m·s^{-1} for a conveyor roller with a plastic casing of 108 mm diameter.

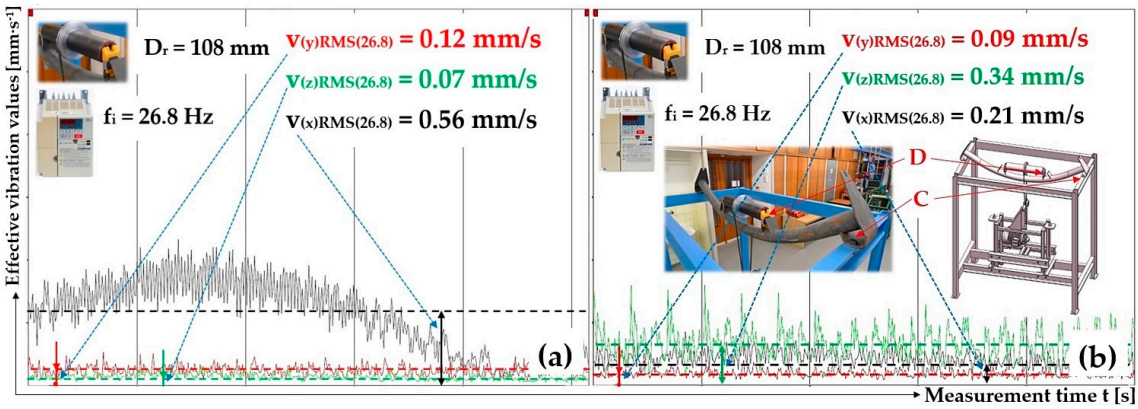

Figure 15. Effective vibration values $v_{(*)RMS(fi)}$ [mm·s^{-1}], plastic roller ϕ108 mm, the circumferential speed of the roller v_r = 2.5 m·s^{-1}, plastic trestle, **(a)** measuring point C, **(b)** measuring point D.

Preprints (www.preprints.org) | NOT PEER-REVIEWED | Posted: 22 November 2023 doi:10.20944/preprints202311.1342.v1

Table 7 indicates effective vibration velocity values $v_{(*)RMS(fi)}$ [mm·s^{-1}], which have been read from the DEWESoft X measurement software, for the vibration measurements of a conveyor roller with a diameter of 133 mm plastic casing at the measuring points A and B for a fixed conveyor idler with plastic brackets.

Table 7. Roller axle placement—plastic trestle, measuring points A and B, roller casing—plastic, D_r = 133 mm.

f_i	n_r	v_r	Measuring point „A"			Measuring point „B"		
			$V_{(x)RMS(fi)}$	$V_{(y)RMS(fi)}$	$V_{(z)RMS(fi)}$	$V_{(x)RMS(fi)}$	$V_{(y)RMS(fi)}$	$V_{(z)RMS(fi)}$
[Hz]	[min^{-1}]	[m·s^{-1}]	[mm·s^{-1}]					
50	824	5.74	0.70	0.37	0.21	0.51	0.29	0.89
33.7	555	3.86	0.46	0.36	0.15	0.50	0.28	0.85
21.8	360	2.51	0.20 [1]	0.21 [1]	0.09 [1]	0.24 [2]	0.13 [2]	0.58 [2]
10.9	179	1.25	0.07	0.11	0.06	0.10	0.08	0.18

[1] see Figure 16a, [2] see Figure 16b.

Figure 16 indicates the measured effective values of the vibration speed $v_{(*)RMS(50)}$ [mm·s^{-1}] in the "x", "y" and "z" axes of the selected coordinate system at circumferential speed v_r = 2.5 m·s^{-1} for a conveyor roller with a plastic casing of 133 mm diameter.

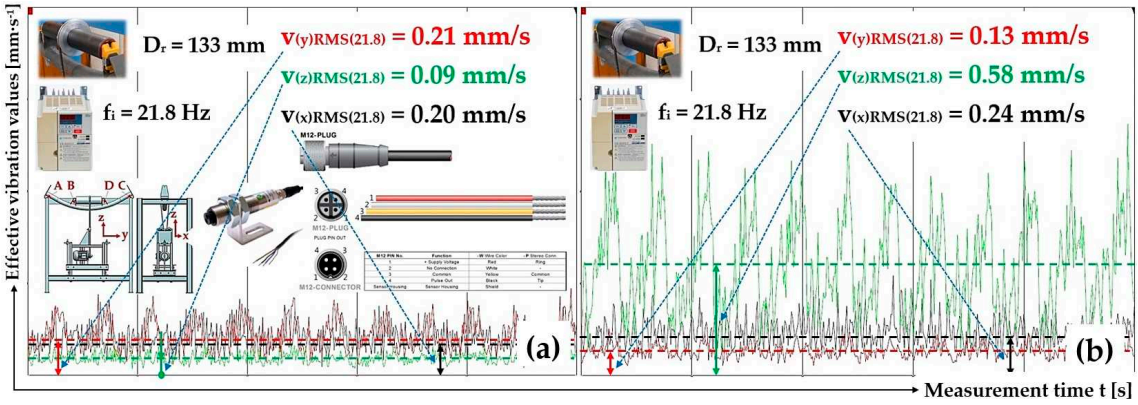

Figure 16. Effective vibration values $v_{(*)RMS(fi)}$ [mm·s^{-1}], plastic roller ϕ133 mm, the circumferential speed of the roller v_r = 2.5 m·s^{-1}, plastic trestle, **(a)** measuring point A, **(b)** measuring point B.

Table 8 indicates effective vibration velocity values $v_{(*)RMS(fi)}$ [mm·s^{-1}], which have been read from the DEWESoft X measurement software, for the vibration measurements of a conveyor roller with a diameter of 133 mm plastic casing at the measuring points C and D for a fixed conveyor idler with plastic brackets.

Table 8. Roller axle placement—plastic trestle, measuring points C and D, roller casing—plastic, D_r = 133 mm.

f_i	n_r	v_r	Measuring point „C"			Measuring point „D"		
			$V_{(x)RMS(fi)}$	$V_{(y)RMS(fi)}$	$V_{(z)RMS(fi)}$	$V_{(x)RMS(fi)}$	$V_{(y)RMS(fi)}$	$V_{(z)RMS(fi)}$
[Hz]	[min^{-1}]	[m·s^{-1}]	[mm·s^{-1}]					
50	825	5.75	0.46	0.46	0.19	0.66	0.43	1.11
33.7	555	3.86	0.73	0.35	0.11	0.55	0.34	0.88
21.8	360	2.50	0.18 [1]	0.20 [1]	0.09 [1]	0.27 [2]	0.13 [2]	0.68 [2]
10.9	179	1.25	0.08	0.09	0.06	0.10	0.08	0.19

[1] see Figure 17a, [2] see Figure 17b.

Preprints (www.preprints.org) | NOT PEER-REVIEWED | Posted: 22 November 2023 doi:10.20944/preprints202311.1342.v1

Figure 17 indicates the measured effective values of the vibration speed $v_{(*)RMS(50)}$ [mm·s^{-1}] in the "x", "y" and "z" axes of the selected coordinate system at circumferential speed v_r = 2.5 m·s^{-1} for a conveyor roller with a plastic casing of 133 mm diameter.

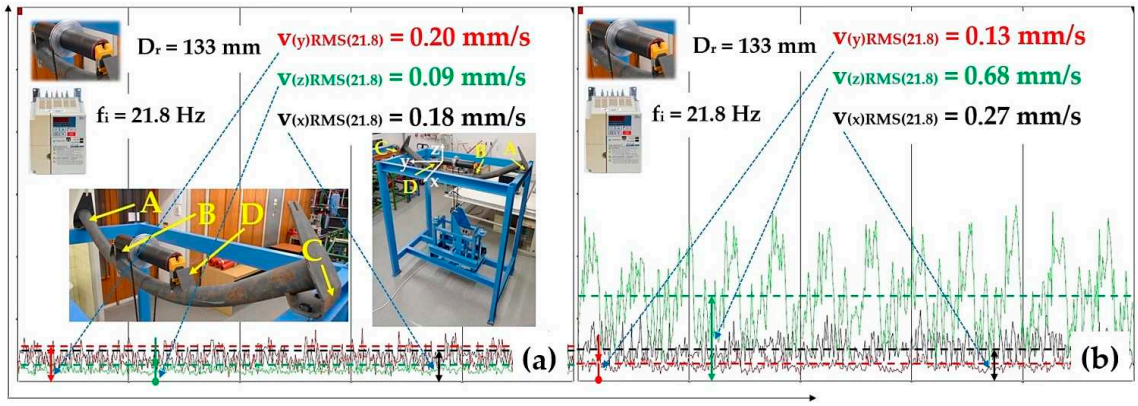

Figure 17. Effective vibration values $v_{(*)RMS(fi)}$ [mm·s^{-1}], plastic roller ϕ133 mm, the circumferential speed of the roller v_r = 2.5 m·s^{-1}, plastic trestle, **(a)** measuring point C, **(b)** measuring point D.

3.2. The Plastic Trestle of a Fixed Conveyor Idler, the Steel Casing of the Conveyor Roller

Table 9 displays the effective vibration velocity values $v_{(*)RMS(fi)}$ [mm·s^{-1}] that were read from the DEWESoft X measurement software provided for the vibration measurements of a steel casing roller with a diameter of 89 mm. These were taken in measuring points A and B of the conveyor idler with plastic brackets on our laboratory device.

Table 9. Roller axles placement—plastic trestle, measuring points A and B, roller casing—steel, D_r = 89 mm.

f_i	n_r	v_r	Measuring point "A"			Measuring point "B"		
			V(x)RMS(fi)	V(y)RMS(fi)	V(z)RMS(fi)	V(x)RMS(fi)	V(y)RMS(fi)	V(z)RMS(fi)
[Hz]	[min^{-1}]	[m·s^{-1}]	[mm·s^{-1}]					
50	823	3.84	0.54 [1]	0.20 [1]	0.11 [1]	0.33 [2]	0.36 [2]	0.46 [2]
32.3	533	2.48	1.93	0.46	0.16	1.32	0.60	0.56
16.1	266	1.24	0.22	0.10	0.08	0.24	0.12	0.21

[1] see Figure 18a, [2] see Figure 18b.

Figure 18. indicates the measured effective values of the vibration speed $v_{(*)RMS(50)}$ [mm·s^{-1}] in the "x", "y" and "z" axes of the selected coordinate system at circumferential speed v_r = 3.84 m·s^{-1} for a conveyor roller with a steel casing of 89 mm diameter. Vibration sensors have been placed at measuring points A and B.

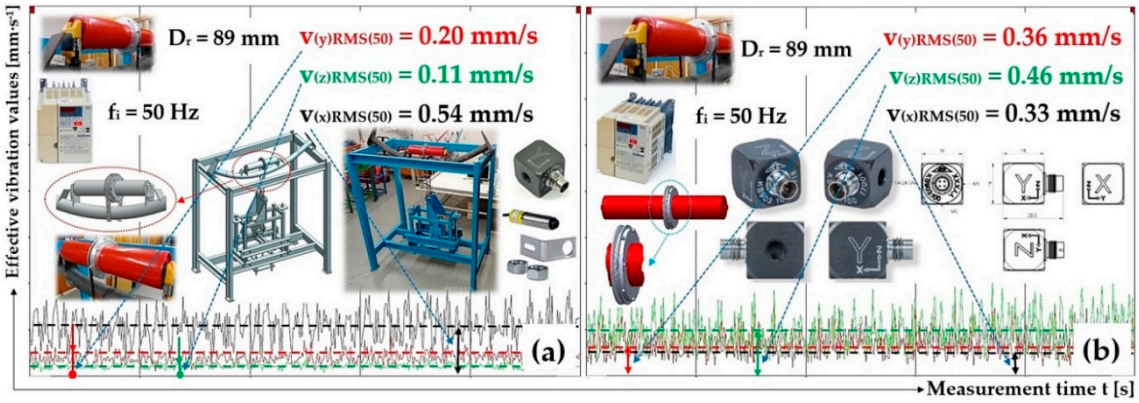

Figure 18. Effective vibration values $v_{(*)RMS(fi)}$ [mm·s^{-1}], stell roller ϕ89 mm, the circumferential speed of the roller v_r = 3.84 m·s^{-1}, plastic trestle, **(a)** measuring point A, **(b)** measuring point B.

Preprints (www.preprints.org) | NOT PEER-REVIEWED | Posted: 22 November 2023 doi:10.20944/preprints202311.1342.v1

Table 10 indicates effective vibration velocity values $v_{(*)RMS(fi)}$ [mm·s^{-1}], which have been read from the DEWESoft X measurement software, for the vibration measurements of a conveyor roller with a diameter of 89 mm steel casing at the measuring points C and D for a fixed conveyor idler with plastic brackets.

Table 10. Roller axles placement—plastic trestle, measuring points C and D, roller casing—steel, D_r = 89 mm.

f_i	n_r	v_r	Measuring point "C"			Measuring point „D"		
			V(x)RMS(fi)	V(y)RMS(fi)	V(z)RMS(fi)	V(x)RMS(fi)	V(y)RMS(fi)	V(z)RMS(fi)
[Hz]	[min^{-1}]	[m·s^{-1}]	[mm·s^{-1}]					
50	823	3.84	1.09 [1]	0.18 [1]	0.26 [1]	0.43 [2]	0.28 [2]	0.46 [2]
32.3	533	2.48	0.81	0.51	0.22	0.70	0.52	0.52
16.12	266	1.24	0.17	0.10	0.09	0.11	0.07	0.18

[1] see Figure 19a, [2] see Figure 19b.

Figure 19 indicates the measured effective values of the vibration speed $v_{(*)RMS(50)}$ [mm·s^{-1}] in the "x", "y" and "z" axes of the selected coordinate system at circumferential speed v_r = 3.84 m·s^{-1} for a conveyor roller with a steel casing of 89 mm diameter. Vibration sensors have been placed at measuring points C and D.

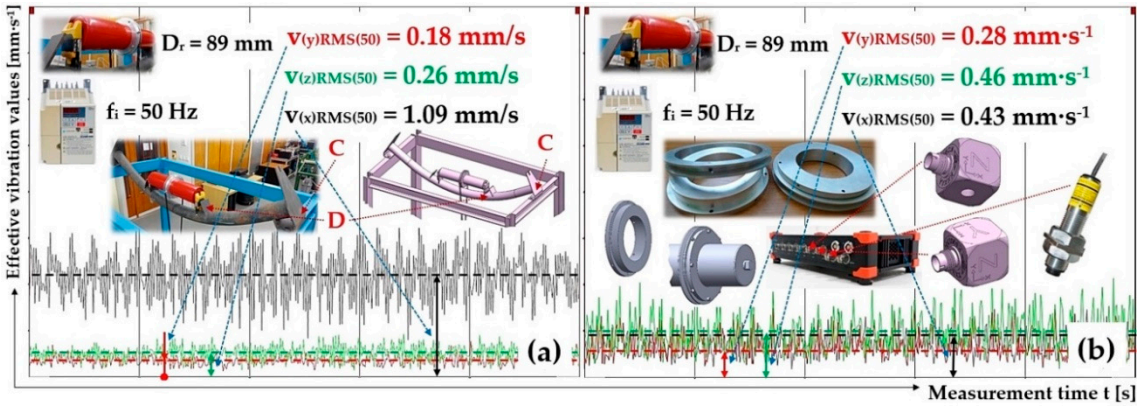

Figure 19. Effective vibration values $v_{(*)RMS(fi)}$ [mm·s^{-1}], stell roller ϕ89 mm, the circumferential speed of the roller v_r = 3.84 m·s^{-1}, plastic trestle, **(a)** measuring point C, **(b)** measuring point D.

Table 11 indicates effective vibration velocity values $v_{(*)RMS(fi)}$ [mm·s^{-1}], which have been read from the DEWESoft X measurement software, for the vibration measurements of a conveyor roller with a diameter of 108 mm steel casing at the measuring points A and B for a fixed conveyor idler with plastic brackets.

Table 11. Roller axles placement—plastic trestle, measuring points A and B, roller casing—steel, D_r = 108 mm.

f_i	n_r	v_r	Measuring point "A"			Measuring point "B"		
			V(x)RMS(fi)	V(y)RMS(fi)	V(z)RMS(fi)	V(x)RMS(fi)	V(y)RMS(fi)	V(z)RMS(fi)
[Hz]	[min^{-1}]	[m·s^{-1}]	[mm·s^{-1}]					
50	826	4.67	0.75	0.24	0.15	0.39	0.19	0.48
41.4	682	3.86	0.36	0.31	0.12	0.32	0.18	0.56
26.84	442	2.5	0.60 [1]	0.11 [1]	0.07 [1]	0.20 [2]	0.12 [2]	0.32 [2]
13.36	220	1.25	0.12	0.08	0.08	0.10	0.08	0.14

[1] see Figure 20a, [2] see Figure 20b.

Preprints (www.preprints.org) | NOT PEER-REVIEWED | Posted: 22 November 2023 doi:10.20944/preprints202311.1342.v1

Figure 20 indicates the measured effective values of the vibration speed $v_{(*)RMS(50)}$ [mm·s^{-1}] in the "x", "y" and "z" axes of the selected coordinate system at circumferential speed v_r = 2.5 m·s^{-1} for a conveyor roller with a steel casing of 108 mm diameter. Vibration sensors have been placed at measuring points A and B.

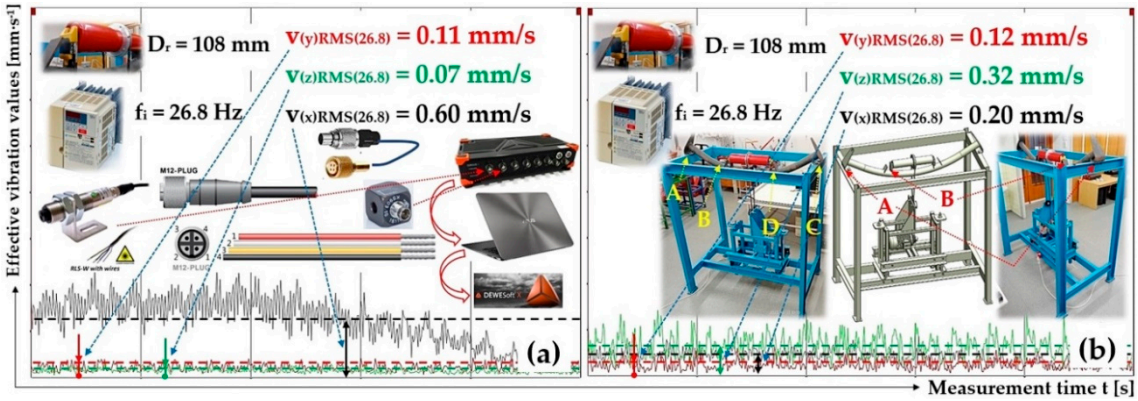

Figure 20. Effective vibration values $v_{(*)RMS(fi)}$ [mm·s^{-1}], stell roller ϕ108 mm, the circumferential speed of the roller v_r = 2.5 m·s^{-1}, plastic trestle, **(a)** measuring point A, **(b)** measuring point B.

Table 12 indicates effective vibration velocity values $v_{(*)RMS(fi)}$ [mm·s^{-1}], which have been read from the DEWESoft X measurement software, for the vibration measurements of a conveyor roller with a diameter of 108 mm steel casing at the measuring points C and D for a fixed conveyor idler with plastic brackets.

Table 12. Roller axles placement—plastic trestle, measuring points C and D, roller casing—steel, D_r = 108 mm.

f_i	n_r	v_r	Measuring point "C"			Measuring point "D"		
			$V_{(x)RMS(fi)}$	$V_{(y)RMS(fi)}$	$V_{(z)RMS(fi)}$	$V_{(x)RMS(fi)}$	$V_{(y)RMS(fi)}$	$V_{(z)RMS(fi)}$
[Hz]	[min^{-1}]	[m·s^{-1}]	[mm·s^{-1}]					
50	826	4.67	1.40	0.20	0.31	0.38	0.19	0.44
41.34	681	3.85	1.27	0.25	0.28	0.61	0.19	0.52
26.85	443	2.5	0.67 [1]	0.14 [1]	0.15 [1]	0.26 [2]	0.12 [2]	0.30 [2]
13.37	220	1.25	0.11	0.12	0.09	0.08	0.07	0.13

[1] see Figure 21a, [2] see Figure 21b.

Figure 21 indicates the measured effective values of the vibration speed $v_{(*)RMS(50)}$ [mm·s^{-1}] in the "x", "y" and "z" axes of the selected coordinate system at circumferential speed v_r = 2.5 m·s^{-1} for a conveyor roller with a steel casing of 108 mm diameter. Vibration sensors have been placed at measuring points C and D.

Preprints (www.preprints.org) | NOT PEER-REVIEWED | Posted: 22 November 2023 doi:10.20944/preprints202311.1342.v1

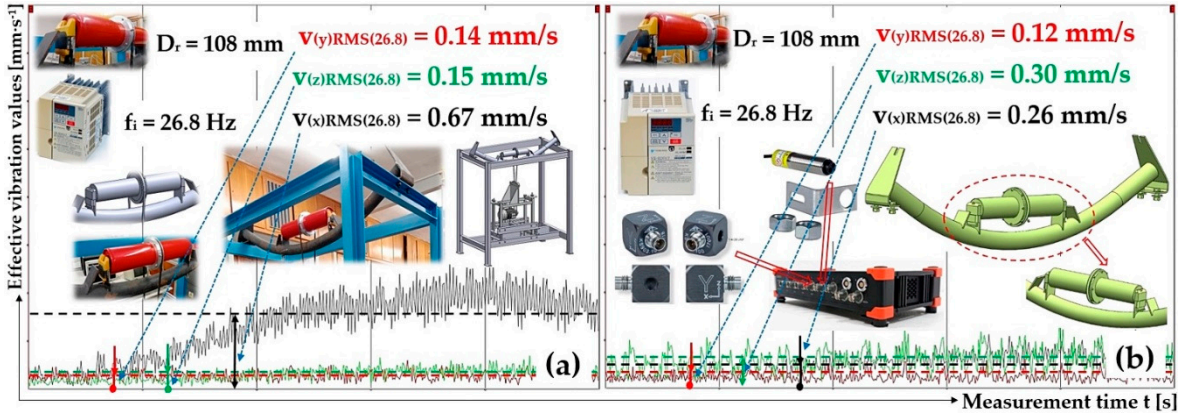

Figure 21. Effective vibration values $v_{(*)RMS(fi)}$ [mm·s^{-1}], stell roller ϕ108 mm, the circumferential speed of the roller v_r = 2.5 m·s^{-1}, plastic trestle, **(a)** measuring point C, **(b)** measuring point D.

Table 13 indicates effective vibration velocity values $v_{(*)RMS(fi)}$ [mm·s^{-1}], which have been read from the DEWESoft X measurement software, for the vibration measurements of a conveyor roller with a diameter of 133 mm steel casing at the measuring points A and B for a fixed conveyor idler with plastic brackets.

Table 13. Roller axles placement—plastic trestle, measuring points A and B, roller casing—steel, D_r = 133 mm.

f_i	n_r	v_r	Measuring point "A"			Measuring point "B"		
			V(x)RMS(fi)	V(y)RMS(fi)	V(z)RMS(fi)	V(x)RMS(fi)	V(y)RMS(fi)	V(z)RMS(fi)
[Hz]	[min^{-1}]	[m·s^{-1}]	[mm·s^{-1}]					
50	825	5.75	0.47	0.24	0.11	0.35	0.24	0.55
33.64	554	3.86	0.64	0.17	0.10	0.48	0.18	0.37
21.92	361	2.52	0.23 [1]	0.12 [1]	0.07 [1]	0.21 [2]	0.13 [2]	0.26 [2]
10.89	179	1.25	0.19	0.09	0.07	0.14	0.09	0.16

[1] see Figure 22a, [2] see Figure 22b.

Figure 22 indicates the measured effective values of the vibration speed $v_{(*)RMS(50)}$ [mm·s^{-1}] in the "x", "y" and "z" axes of the selected coordinate system at circumferential speed v_r = 2.5 m·s^{-1} for a conveyor roller with a steel casing of 133 mm diameter. Vibration sensors have been placed at measuring points A and B.

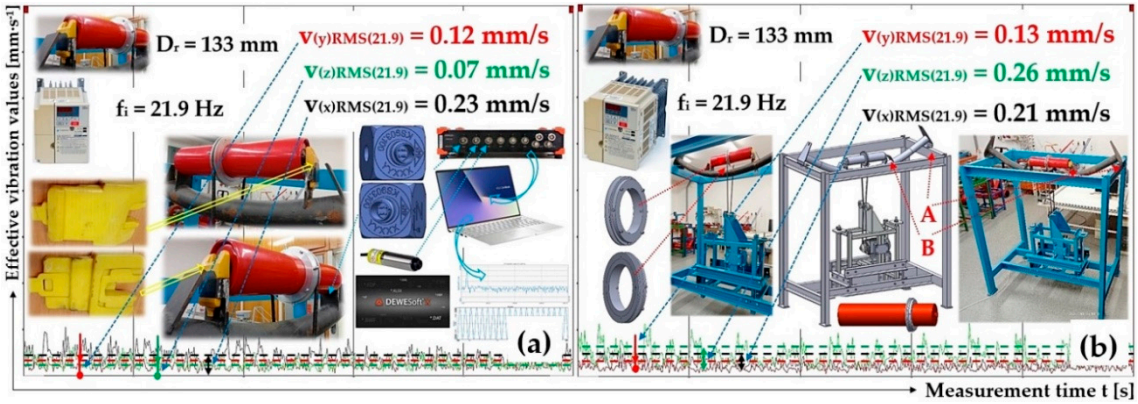

Figure 22. Effective vibration values $v_{(*)RMS(fi)}$ [mm·s^{-1}], stell roller ϕ133 mm, the circumferential speed of the roller v_r = 2.5 m·s^{-1}, plastic trestle, **(a)** measuring point A, **(b)** measuring point B.

Table 14 indicates effective vibration velocity values $v_{(*)RMS(fi)}$ [mm·s^{-1}], which have been read from the DEWESoft X measurement software, for the vibration measurements of a conveyor roller

Preprints (www.preprints.org) | NOT PEER-REVIEWED | Posted: 22 November 2023 doi:10.20944/preprints202311.1342.v1

with a diameter of 133 mm steel casing at the measuring points C and D for a fixed conveyor idler with plastic brackets.

Table 14. Roller axles placement—plastic trestle, measuring points C and D, roller casing—steel, D_r = 133 mm.

f_i	n_r	v_r	Measuring point "C"			Measuring point "D"		
			$V_{(x)RMS(fi)}$	$V_{(y)RMS(fi)}$	$V_{(z)RMS(fi)}$	$V_{(x)RMS(fi)}$	$V_{(y)RMS(fi)}$	$V_{(z)RMS(fi)}$
[Hz]	[min^{-1}]	[m·s^{-1}]	[mm·s^{-1}]					
50	825	5.75	0.49	0.24	0.18	0.27	0.19	0.48
33.67	555	3.87	0.32	0.18	0.17	0.30	0.14	0.31
21.87	361	2.51	0.21 [1]	0.11 [1]	0.14 [1]	0.13 [2]	0.09 [2]	0.23 [2]
10.89	179	1.25	0.11	0.07	0.08	0.08	0.06	0.14

[1] see Figure 23a, [2] see Figure 23b.

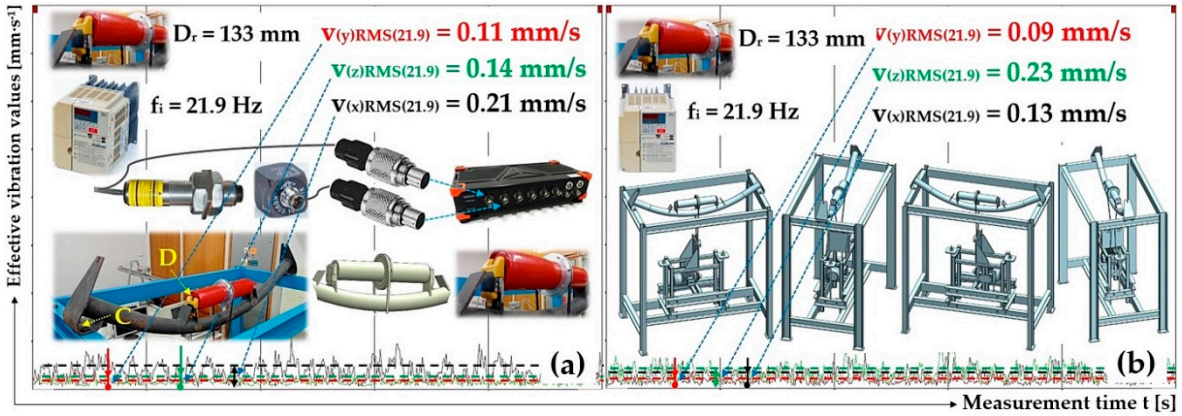

Figure 23. Effective vibration values $v_{(*)RMS(fi)}$ [mm·s^{-1}], stell roller ϕ133 mm, the circumferential speed of the roller v_r = 2.5 m·s^{-1}, plastic trestle, **(a)** measuring point C, **(b)** measuring point D.

3.3. The steel Trestle of the Fixed Conveyor Idler, the Plastic Casing of the Conveyor Roller

Table 15 lists the effective vibration velocity values $v_{(*)RMS(fi)}$ [mm·s^{-1}] that were read from the DEWESoft X measurement software for the vibration values of a conveyor roller with a diameter of 89 mm plastic casing taken in measuring points A and B of a fixed conveyor idler with steel trestles, see Figure 10a, of the laboratory device (Figure 11).

Table 15. Roller axles placement—steel trestle, measuring points A and B, roller casing—plastic, D_r = 89 mm.

f_i	n_r	v_r	Measuring point „A"			Measuring point „B"		
			$V_{(x)RMS(fi)}$	$V_{(y)RMS(fi)}$	$V_{(z)RMS(fi)}$	$V_{(x)RMS(fi)}$	$V_{(y)RMS(fi)}$	$V_{(z)RMS(fi)}$
[Hz]	[min^{-1}]	[m·s^{-1}]	[mm·s^{-1}]				[mm·s^{-1}]	
50	824	3.84	0.25 [1]	0.40 [1]	0.24 [1]	0.77 [2]	0.24 [2]	1.13 [2]
32.33	533	2.48	0.92	0.25	0.17	1.02	0.14	0.81
16.14	266	1.24	0.09	0.14	0.15	0.28	0.13	0.32

[1] see Figure 24a, [2] see Figure 24b.

Figure 24 shows the measured RMS values for the vibration velocity $v_{(*)RMS(50)}$ [mm·s^{-1}] in axes "x", "y" and "z" for the selected coordinate system at circumferential speed v_r = 3.84 m·s^{-1} of the conveyor roller with a plastic casing with an 89 mm diameter. With regard to the scope of the paper, the measured graphs of the effective values of vibration velocities $v_{(*)RMS(fi)}$ [mm·s^{-1}] are not presented in this paper for circumferential speeds v_r = 2.5 m·s^{-1} and v_r = 1.25 m·s^{-1}.

Preprints (www.preprints.org) | NOT PEER-REVIEWED | Posted: 22 November 2023 doi:10.20944/preprints202311.1342.v1

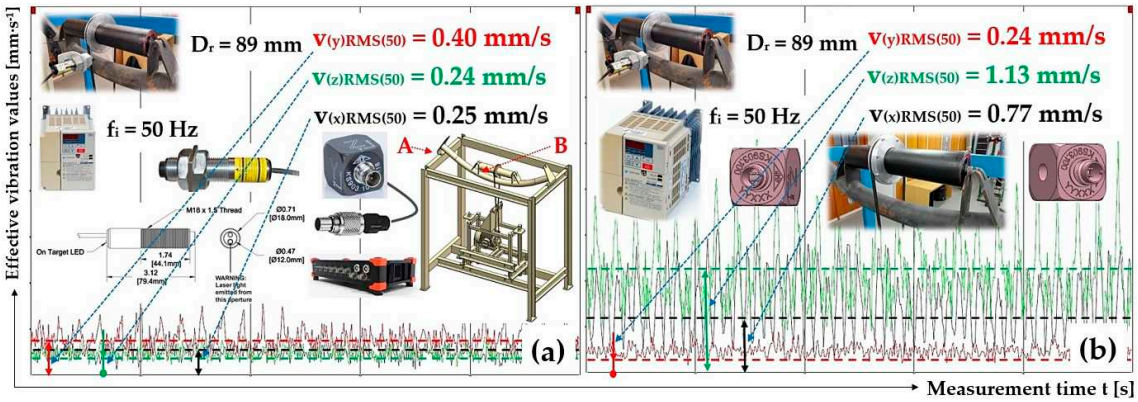

Figure 24. Effective vibration values $v_{(*)RMS(fi)}$ [mm·s^{-1}], plastic roller ϕ89 mm, the circumferential speed of the roller v_r = 3.85 m·s^{-1}, steel trestle, **(a)** measuring point A, **(b)** measuring point B.

Table 16 indicates effective vibration velocity values $v_{(*)RMS(fi)}$ [mm·s^{-1}], which have been read from the DEWESoft X measurement software, for the vibration measurements of a conveyor roller with a diameter of 89 mm plastic casing at the measuring points C and D for a fixed conveyor idler with steel brackets.

Table 16. Roller axles placement—steel trestle, measuring points C and D roller casing—plastic, D_r = 89 mm.

f_i	n_r	v_r	Measuring point „C"			Measuring point „D"		
			V(x)RMS(fi)	V(y)RMS(fi)	V(z)RMS(fi)	V(x)RMS(fi)	V(y)RMS(fi)	V(z)RMS(fi)
[Hz]	[min^{-1}]	[m·s^{-1}]	[mm·s^{-1}]					
50	826	3.85	0.28 [1]	0.37 [1]	0.15 [1]	0.77 [2]	0.27 [2]	1.04 [2]
32.35	533	2.48	0.26	0.28	0.12	0.89	0.17	0.79
16.15	266	1.24	0.11	0.17	0.13	0.31	0.14	0.33

[1] see Figure 25a, [2] see Figure 25b.

Figure 25 indicates the measured effective values of the vibration speed $v_{(*)RMS(50)}$ [mm·s^{-1}] in the "x", "y" and "z" axes of the selected coordinate system at circumferential speed v_r = 3.85 m·s^{-1} for a conveyor roller with a plastic casing of 89 mm diameter. Vibration sensors have been placed at measuring points C and D.

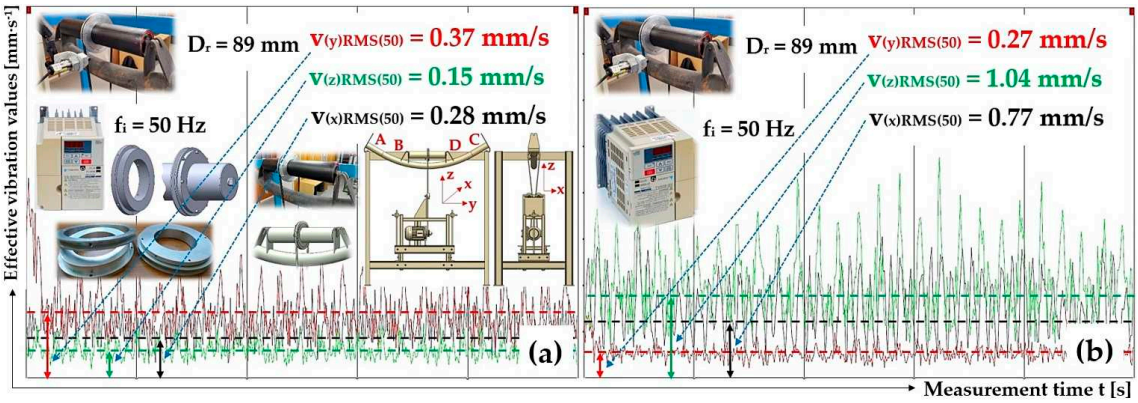

Figure 25. Effective vibration values $v_{(*)RMS(fi)}$ [mm·s^{-1}], plastic roller ϕ89 mm, the circumferential speed of the roller v_r = 3.85 m·s^{-1}, steel trestle, **(a)** measuring point C, **(b)** measuring point D.

Table 17 indicates effective vibration velocity values $v_{(*)RMS(fi)}$ [mm·s^{-1}], which have been read from the DEWESoft X measurement software, for the vibration measurements of a conveyor roller with a diameter of 108 mm plastic casing at the measuring points A and B for a fixed conveyor idler with steel brackets.

Preprints (www.preprints.org) | NOT PEER-REVIEWED | Posted: 22 November 2023 doi:10.20944/preprints202311.1342.v1

Table 17. Roller axles placement—steel trestle, measuring points A and B roller casing—plastic, D_r = 108 mm.

f_i	n_r	v_r	Measuring point „A“			Measuring point „B“		
			$V_{(x)RMS(fi)}$	$V_{(y)RMS(fi)}$	$V_{(z)RMS(fi)}$	$V_{(x)RMS(fi)}$	$V_{(y)RMS(fi)}$	$V_{(z)RMS(fi)}$
[Hz]	[min^{-1}]	[m·s^{-1}]	[mm·s^{-1}]					
50	825	4.66	0.44	0.53	0.36	0.66	0.32	2.16
41.24	680	3.84	0.28	0.41	0.22	0.76	0.32	1.33
26.73	441	2.50	0.33 [1]	0.26 [1]	0.14 [1]	0.78 [2]	0.20 [2]	0.81 [2]
13.34	220	1.24	0.08	0.13	0.06	0.17	0.10	0.32

[1] see Figure 26a, [2] see Figure 26b.

Figure 26 indicates the measured effective values of the vibration speed $v_{(*)RMS(50)}$ [mm·s^{-1}] in the "x", "y" and "z" axes of the selected coordinate system at circumferential speed v_r = 2.5 m·s^{-1} for a conveyor roller with a plastic casing of 108 mm diameter. Vibration sensors have been placed at measuring points A and B.

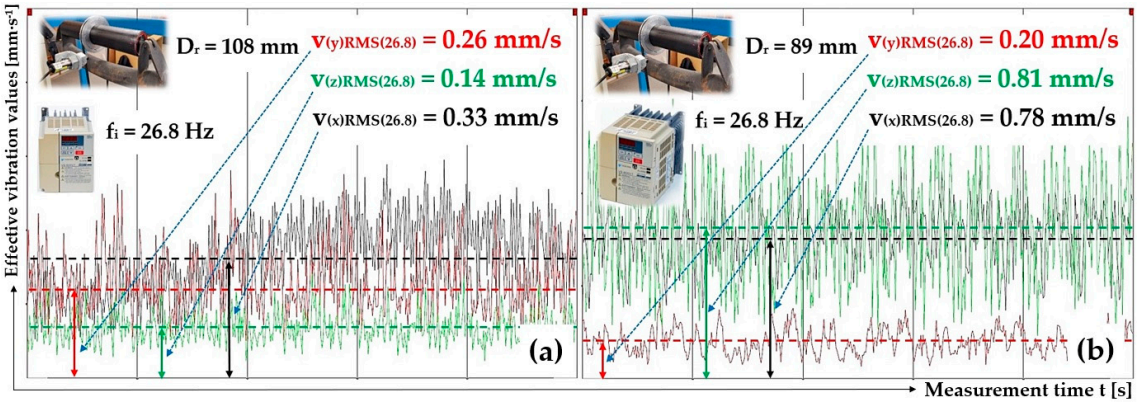

Figure 26. Effective vibration values $v_{(*)RMS(fi)}$ [mm·s^{-1}], plastic roller ϕ108 mm, the circumferential speed of the roller v_r = 2.5 m·s^{-1}, steel trestle, **(a)** measuring point A, **(b)** measuring point B.

Table 18 indicates effective vibration velocity values $v_{(*)RMS(fi)}$ [mm·s^{-1}], which have been read from the DEWESoft X measurement software, for the vibration measurements of a conveyor roller with a diameter of 108 mm plastic casing at the measuring points C and D for a fixed conveyor idler with steel brackets.

Table 18. Roller axles placement—steel trestle, measuring points C and D roller casing—plastic, D_r = 108 mm.

f_i	n_r	v_r	Measuring point „C“			Measuring point „D“		
			$V_{(x)RMS(fi)}$	$V_{(y)RMS(fi)}$	$V_{(z)RMS(fi)}$	$V_{(x)RMS(fi)}$	$V_{(y)RMS(fi)}$	$V_{(z)RMS(fi)}$
[Hz]	[min^{-1}]	[m·s^{-1}]	[mm·s^{-1}]					
50	823	4.65	0.58	0.86	0.23	0.61	0.45	2.54
41.29	681	3.85	0.66	0.48	0.18	0.76	0.40	1.30
26.68	440	2.49	0.35 [1]	0.24 [1]	0.11 [1]	0.63 [1]	0.18 [1]	0.64 [1]
13.35	220	1.24	0.08	0.13	0.06	0.14	0.09	0.32

[1] see Figure 27a, [2] see Figure 27b.

Figure 27 indicates the measured effective values of the vibration speed $v_{(*)RMS(50)}$ [mm·s^{-1}] in the "x", "y" and "z" axes of the selected coordinate system at circumferential speed v_r = 2.5 m·s^{-1} for a conveyor roller with a plastic casing of 108 mm diameter. Vibration sensors have been placed at measuring points C and D.

Preprints (www.preprints.org) | NOT PEER-REVIEWED | Posted: 22 November 2023 doi:10.20944/preprints202311.1342.v1

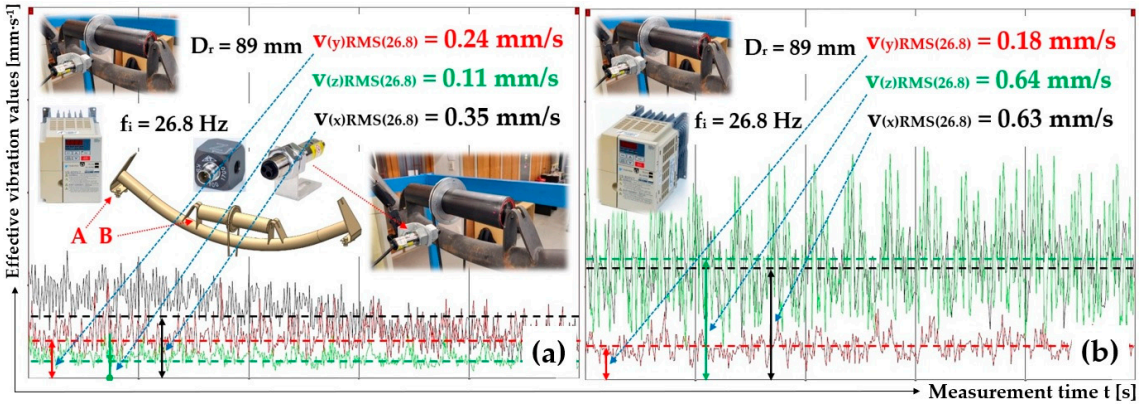

Figure 27. Effective vibration values $v_{(*)RMS(fi)}$ [mm·s^{-1}], plastic roller ϕ108 mm, the circumferential speed of the roller v_r = 2.5 m·s^{-1}, steel trestle, **(a)** measuring point C, **(b)** measuring point D.

Table 19 indicates effective vibration velocity values $v_{(*)RMS(fi)}$ [mm·s^{-1}], which have been read from the DEWESoft X measurement software, for the vibration measurements of a conveyor roller with a diameter of 133 mm plastic casing at the measuring points A and B for a fixed conveyor idler with steel brackets.

Table 19. Roller axles placement—steel trestle, measuring points A and B roller casing—plastic, D_r = 133 mm.

f_i	n_r	v_r	Measuring point „A"			Measuring point „B"		
			V(x)RMS(fi)	V(y)RMS(fi)	V(z)RMS(fi)	V(x)RMS(fi)	V(y)RMS(fi)	V(z)RMS(fi)
[Hz]	[min^{-1}]	[m·s^{-1}]	[mm·s^{-1}]					
50	825	5.75	0.44	0.66	0.41	0.76	0.41	2.31
33.48	552	3.84	0.46	0.43	0.20	0.57	0.38	0.97
21.83	360	2.51	0.13 [1]	0.25 [1]	0.14 [1]	0.35 [2]	0.21 [2]	0.61 [2]
10.84	179	1.24	0.08	0.12	0.09	0.16	0.09	0.20

[1] see Figure 28a, [2] see Figure 28b.

Figure 28 indicates the measured effective values of the vibration speed $v_{(*)RMS(50)}$ [mm·s^{-1}] in the "x", "y" and "z" axes of the selected coordinate system at circumferential speed v_r = 2.5 m·s^{-1} for a conveyor roller with a plastic casing of 133 mm diameter. Vibration sensors have been placed at measuring points A and B.

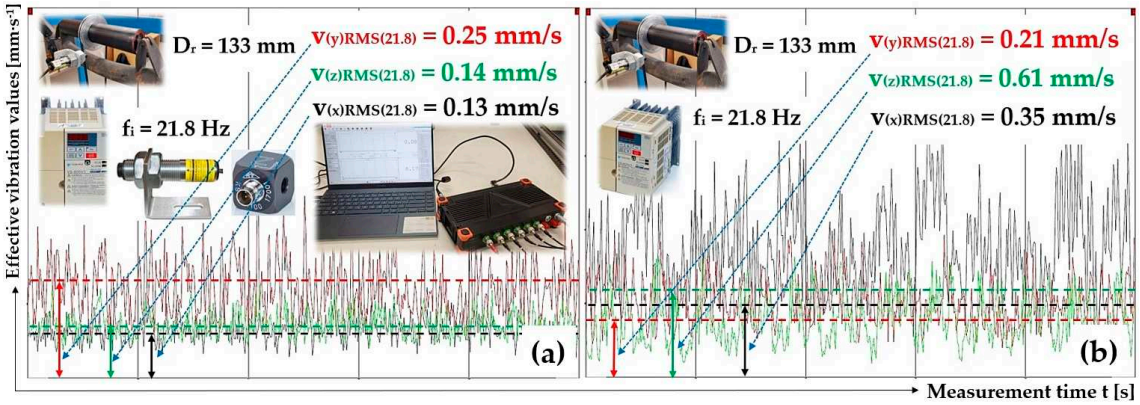

Figure 28. Effective vibration values $v_{(*)RMS(fi)}$ [mm·s^{-1}], plastic roller ϕ133 mm, the circumferential speed of the roller v_r = 2.5 m·s^{-1}, steel trestle, **(a)** measuring point A, **(b)** measuring point B.

Table 20 indicates effective vibration velocity values $v_{(*)RMS(fi)}$ [mm·s^{-1}], which have been read from the DEWESoft X measurement software, for the vibration measurements of a conveyor roller

Preprints (www.preprints.org) | NOT PEER-REVIEWED | Posted: 22 November 2023 doi:10.20944/preprints202311.1342.v1

with a diameter of 133 mm plastic casing at the measuring points A and B for a fixed conveyor idler with steel brackets.

Table 20. Roller axles placement—steel trestle, measuring points C and D roller casing—plastic, D_r = 133 mm.

f_i	n_r	v_r	Measuring point „C“			Measuring point „D“		
			$V_{(x)RMS(fi)}$	$V_{(y)RMS(fi)}$	$V_{(z)RMS(fi)}$	$V_{(x)RMS(fi)}$	$V_{(y)RMS(fi)}$	$V_{(z)RMS(fi)}$
[Hz]	[min^{-1}]	[m·s^{-1}]	[mm·s^{-1}]					
50	824	5.74	0.69	0.68	0.23	0.95	0.39	1.94
33.56	553	3.85	0.49	0.38	0.16	0.63	0.27	0.92
21.84	360	2.51	0.18 [1]	0.23 [1]	0.12 [1]	0.38 [2]	0.18 [2]	0.57 [2]
10.84	179	1.24	0.11	0.15	0.09	0.21	0.10	0.19

[1] see Figure 29a, [2] see Figure 29b.

Figure 29 indicates the measured effective values of the vibration speed $v_{(*)RMS(50)}$ [mm·s^{-1}] in the "x", "y" and "z" axes of the selected coordinate system at circumferential speed v_r = 2.5 m·s^{-1} for a conveyor roller with a plastic casing of 133 mm diameter. Vibration sensors have been placed at measuring points C and D.

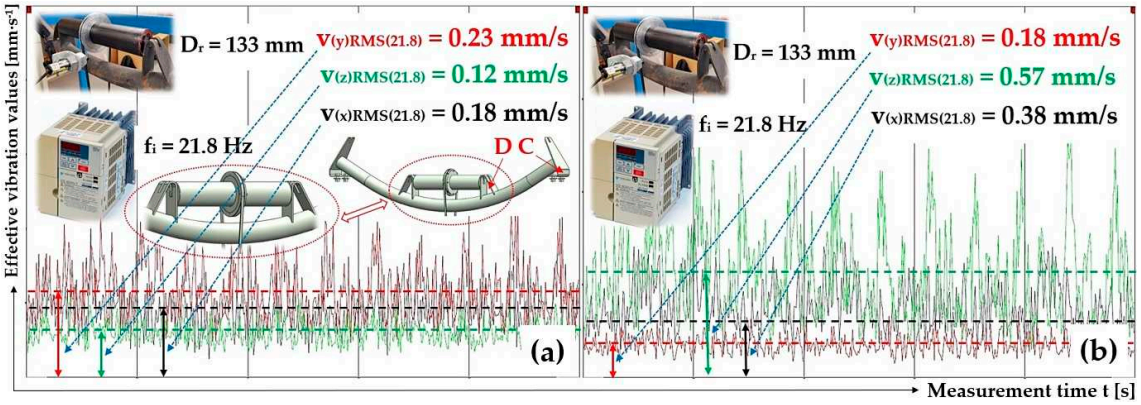

Figure 29. Effective vibration values $v_{(*)RMS(fi)}$ [mm·s^{-1}], plastic roller ϕ133 mm, the circumferential speed of the roller v_r = 2.5 m·s^{-1}, steel trestle, **(a)** measuring point C, **(b)** measuring point D.

3.4. The steel Trestle of the Fixed Conveyor Idler, the Steel Casing of the Conveyor Roller

Table 21 lists the effective vibration velocity values $v_{(*)RMS(fi)}$ [mm·s^{-1}] that have been read from the DEWESoft X software for the vibration values measured on the 89 mm diameter conveyor roller with the steel casing at the measuring points A and B of the fixed conveyor idler. The flattened ends of the conveyor roller axle are supported in the steel trestles of the fixed conveyor idler.

Table 21. Roller axles placement—steel trestle, measuring points A and B roller casing—steel, D_r = 89 mm.

f_i	n_r	v_r	Measuring point „A“			Measuring point „B“		
			$V_{(x)RMS(fi)}$	$V_{(y)RMS(fi)}$	$V_{(z)RMS(fi)}$	$V_{(x)RMS(fi)}$	$V_{(y)RMS(fi)}$	$V_{(z)RMS(fi)}$
[Hz]	[min^{-1}]	[m·s^{-1}]	[mm·s^{-1}]			[mm·s^{-1}]		
50	825	3.84	0.46 [1]	0.38 [1]	0.17 [1]	0.82 [2]	0.20 [2]	1.23 [2]
32.4	534	2.49	0.92	0.57	0.13	0.96	0.57	0.80
16.17	267	1.24	0.09	0.11	0.07	0.21	0.07	0.24

[1] see Figure 30a, [2] see Figure 30b.

Preprints (www.preprints.org) | NOT PEER-REVIEWED | Posted: 22 November 2023 doi:10.20944/preprints202311.1342.v1

Figure 30 indicates the measured effective values of the vibration speed $v_{(*)RMS(50)}$ [mm·s^{-1}] in the "x", "y" and "z" axes of the selected coordinate system at circumferential speed v_r = 3.84 m·s^{-1} for a conveyor roller with a steel casing of 89 mm diameter. Vibration sensors have been placed at measuring points A and B.

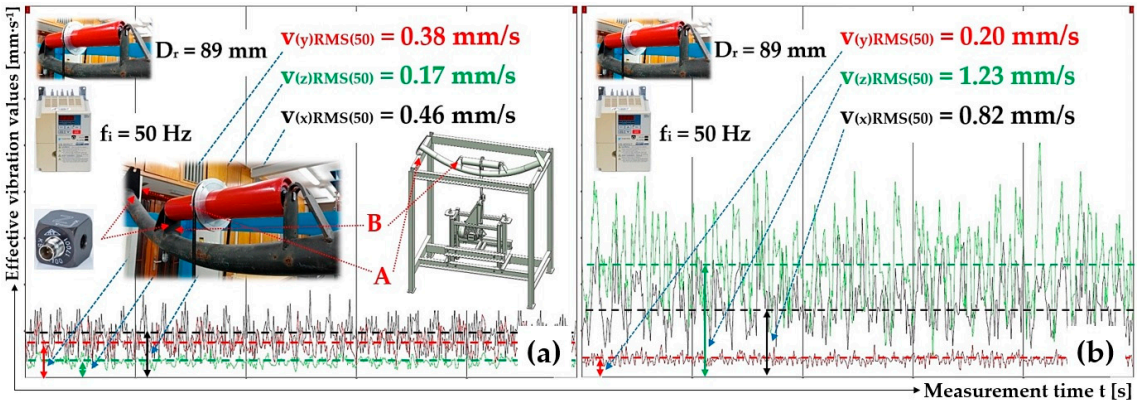

Figure 30. Effective vibration values $v_{(*)RMS(fi)}$ [mm·s^{-1}], steel roller ϕ89 mm, the circumferential speed of the roller v_r = 3.84 m·s^{-1}, steel trestle, **(a)** measuring point A, **(b)** measuring point B.

Table 22 indicates effective vibration velocity values $v_{(*)RMS(fi)}$ [mm·s^{-1}], which have been read from the DEWESoft X measurement software, for the vibration measurements of a conveyor roller with a diameter of 89 mm steel casing at the measuring points A and B for a fixed conveyor idler with steel brackets.

Table 22. Roller axles placement—steel trestle, measuring points C and D roller casing—steel, D_r = 89 mm.

f_i	n_r	v_r	Measuring point „C"			Measuring point „D"		
			V(x)RMS(fi)	V(y)RMS(fi)	V(z)RMS(fi)	V(x)RMS(fi)	V(y)RMS(fi)	V(z)RMS(fi)
[Hz]	[min^{-1}]	[m·s^{-1}]	[mm·s^{-1}]					
50	826	3.85	0.92 [1]	0.36 [1]	0.26 [1]	0.79 [2]	0.18 [2]	1.15 [2]
32.4	534	2.49	0.92	0.57	0.13	0.96	0.57	0.80
16.17	267	1.24	0.09	0.11	0.07	0.21	0.07	0.24

[1] see Figure 31a, [2] see Figure 31b.

Figure 31 indicates the measured effective values of the vibration speed $v_{(*)RMS(50)}$ [mm·s^{-1}] in the "x", "y" and "z" axes of the selected coordinate system at circumferential speed v_r = 3.84 m·s^{-1} for a conveyor roller with a steel casing of 89 mm diameter. Vibration sensors have been placed at measuring points C and D.

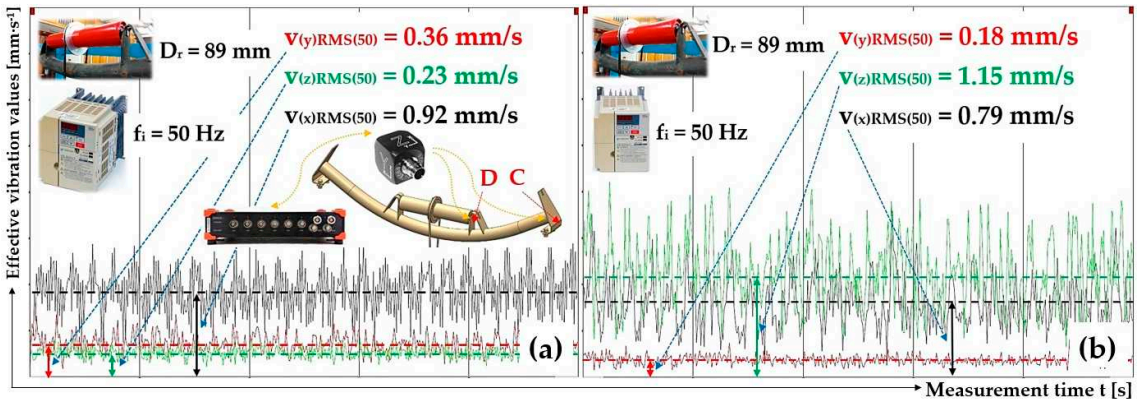

Figure 31. Effective vibration values $v_{(*)RMS(fi)}$ [mm·s^{-1}], steel roller ϕ89 mm, the circumferential speed of the roller v_r = 3.85 m·s^{-1}, steel trestle, **(a)** measuring point C, **(b)** measuring point D.

Preprints (www.preprints.org) | NOT PEER-REVIEWED | Posted: 22 November 2023 doi:10.20944/preprints202311.1342.v1

Table 23 indicates effective vibration velocity values $v_{(*)RMS(fi)}$ [mm·s^{-1}], which have been read from the DEWESoft X measurement software, for the vibration measurements of a conveyor roller with a diameter of 108 mm steel casing at the measuring points A and B for a fixed conveyor idler with steel brackets.

Table 23. Roller axles placement—steel trestle, measuring points A and B roller casing—steel, D_r = 108 mm.

f_i	n_r	v_r	Measuring point „A“			Measuring point „B“		
			V(x)RMS(fi)	V(y)RMS(fi)	V(z)RMS(fi)	V(x)RMS(fi)	V(y)RMS(fi)	V(z)RMS(fi)
[Hz]	[min^{-1}]	[m·s^{-1}]	[mm·s^{-1}]					
50	823	4.65	0.61	0.35	0.15	0.83	0.24	0.94
41.25	680	3.85	0.35	0.36	0.11	0.90	0.24	1.12
26.73	441	2.49	0.38 [1]	0.16 [1]	0.09 [1]	0.44 [2]	0.10 [2]	0.50 [2]
13.30	219	1.24	0.06	0.10	0.05	0.14	0.08	0.25

[1] see Figure 32a, [2] see Figure 32b.

Figure 32 indicates the measured effective values of the vibration speed $v_{(*)RMS(50)}$ [mm·s^{-1}] in the "x", "y" and "z" axes of the selected coordinate system at circumferential speed v_r = 2.5 m·s^{-1} for a conveyor roller with a steel casing of 108 mm diameter. Vibration sensors have been placed at measuring points A and B.

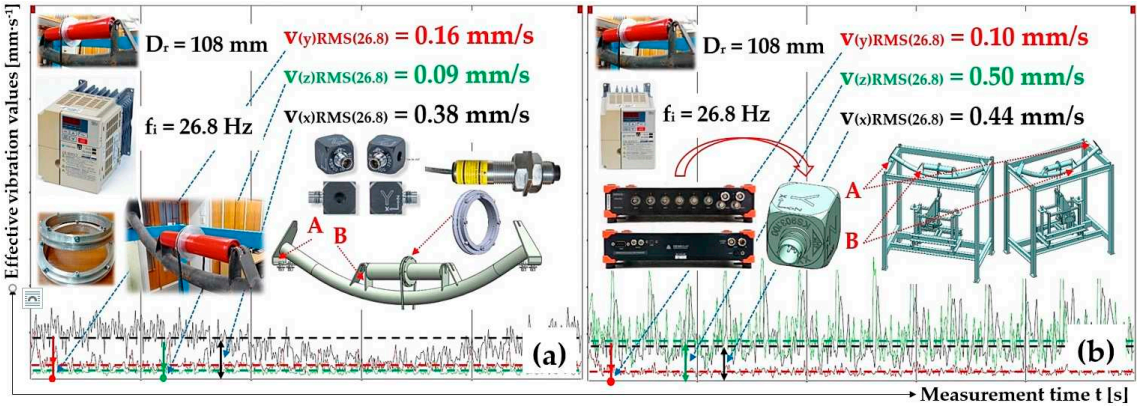

Figure 32. Effective vibration values $v_{(*)RMS(fi)}$ [mm·s^{-1}], steel roller ϕ108 mm, the circumferential speed of the roller v_r = 2.5 m·s^{-1}, steel trestle, **(a)** measuring point A, **(b)** measuring point B.

Table 24 indicates effective vibration velocity values $v_{(*)RMS(fi)}$ [mm·s^{-1}], which have been read from the DEWESoft X measurement software, for the vibration measurements of a conveyor roller with a diameter of 108 mm steel casing at the measuring points C and D for a fixed conveyor idler with steel brackets.

Table 24. Roller axles placement—steel trestle, measuring points C and D roller casing—steel, D_r = 108 mm.

f_i	n_r	v_r	Measuring point „C“			Measuring point „D“		
			V(x)RMS(fi)	V(y)RMS(fi)	V(z)RMS(fi)	V(x)RMS(fi)	V(y)RMS(fi)	V(z)RMS(fi)
[Hz]	[min^{-1}]	[m·s^{-1}]	[mm·s^{-1}]					
50	823	4.66	1.14	0.30	0.28	0.99	0.24	0.84
41.20	679	3.84	1.19	0.40	0.33	1.03	0.33	1.10
26.73	441	2.49	0.46 [1]	0.20 [1]	0.14 [1]	0.52 [2]	0.12 [2]	0.59 [2]
13.32	220	1.24	0.07	0.10	0.07	0.13	0.07	0.21

[1] see Figure 33a, [2] see Figure 33b.

Preprints (www.preprints.org) | NOT PEER-REVIEWED | Posted: 22 November 2023 doi:10.20944/preprints202311.1342.v1

Figure 33 indicates the measured effective values of the vibration speed $v_{(*)RMS(50)}$ [mm·s^{-1}] in the "x", "y" and "z" axes of the selected coordinate system at circumferential speed v_r = 2.5 m·s^{-1} for a conveyor roller with a steel casing of 108 mm diameter. Vibration sensors have been placed at measuring points C and D.

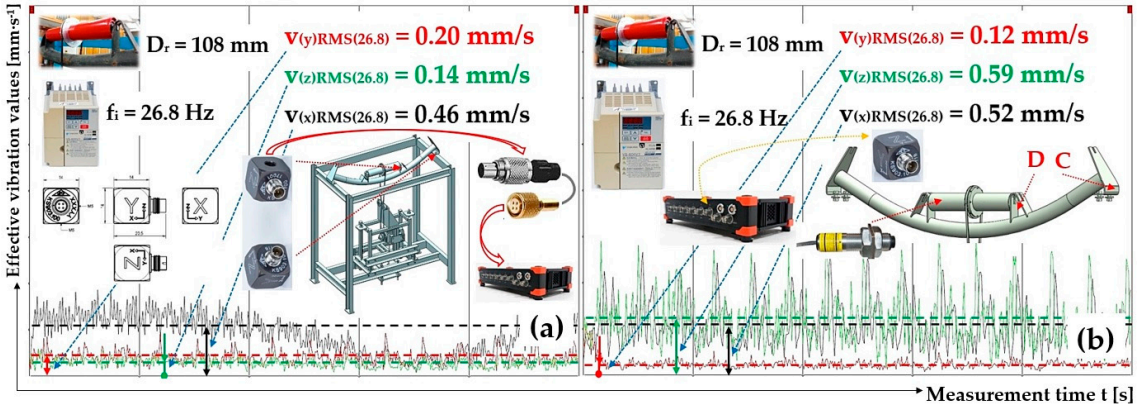

Figure 33. Effective vibration values $v_{(*)RMS(fi)}$ [mm·s^{-1}], steel roller ϕ108 mm, the circumferential speed of the roller v_r = 2.5 m·s^{-1}, steel trestle, **(a)** measuring point C, **(b)** measuring point D.

Table 25 indicates effective vibration velocity values $v_{(*)RMS(fi)}$ [mm·s^{-1}], which have been read from the DEWESoft X measurement software, for the vibration measurements of a conveyor roller with a diameter of 133 mm steel casing at the measuring points A and B for a fixed conveyor idler with steel brackets.

Table 25. Roller axles placement—steel trestle, measuring points A and B roller casing—steel, D_r = 133 mm.

f_i	n_r	v_r	Measuring point „A"			Measuring point „B"		
			V(x)RMS(fi)	V(y)RMS(fi)	V(z)RMS(fi)	V(x)RMS(fi)	V(y)RMS(fi)	V(z)RMS(fi)
[Hz]	[min^{-1}]	[m·s^{-1}]	[mm·s^{-1}]					
50	826	5.75	0.29	0.29	0.13	0.46	0.18	0.87
33.66	555	3.86	0.43	0.21	0.11	0.49	0.14	0.68
21.89	361	2.51	0.14 [1]	0.13 [1]	0.08 [1]	0.26 [2]	0.09 [2]	0.39 [2]
10.87	179	1.25	0.10	0.06	0.11	0.14	0.09	0.18

[1] see Figure 34a, [2] see Figure 34b.

Figure 34 indicates the measured effective values of the vibration speed $v_{(*)RMS(50)}$ [mm·s^{-1}] in the "x", "y" and "z" axes of the selected coordinate system at circumferential speed v_r = 2.5 m·s^{-1} for a conveyor roller with a steel casing of 133 mm diameter. Vibration sensors have been placed at measuring points A and B.

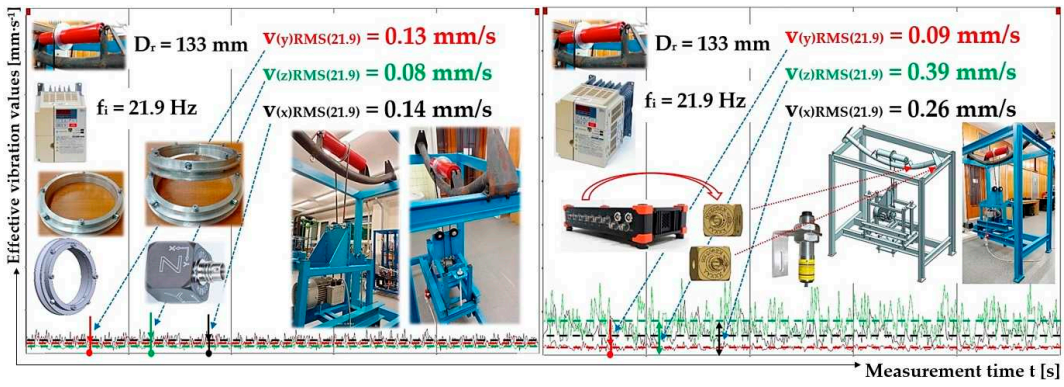

Figure 34. Effective vibration values $v_{(*)RMS(fi)}$ [mm·s^{-1}], steel roller ϕ133 mm, the circumferential speed of the roller v_r = 2.5 m·s^{-1}, steel trestle, **(a)** measuring point A, **(b)** measuring point B.

Preprints (www.preprints.org) | NOT PEER-REVIEWED | Posted: 22 November 2023 doi:10.20944/preprints202311.1342.v1

Table 26 indicates effective vibration velocity values $v_{(*)RMS(fi)}$ [mm·s^{-1}], which have been read from the DEWESoft X measurement software, for the vibration measurements of a conveyor roller with a diameter of 133 mm steel casing at the measuring points A and B for a fixed conveyor idler with steel brackets.

Table 26. Roller axles placement—steel trestle, measuring points C and D roller casing—steel, D_r = 133 mm.

f_i	n_r	v_r	Measuring point „C“			Measuring point „D“		
			V(x)RMS(fi)	V(y)RMS(fi)	V(z)RMS(fi)	V(x)RMS(fi)	V(y)RMS(fi)	V(z)RMS(fi)
[Hz]	[min^{-1}]	[m·s^{-1}]	[mm·s^{-1}]					
50	824	5.74	0.33	0.30	0.17	0.42	0.20	0.83
33.59	554	3.86	0.26	0.21	0.12	0.33	0.14	0.59
21.87	361	2.51	0.23 [1]	0.15 [1]	0.10 [1]	0.23 [2]	0.10 [2]	0.40 [2]
10.87	179	1.25	0.10	0.14	0.09	0.11	0.09	0.18

[1] see Figure 35a, [2] see Figure 35b.

Figure 35 indicates the measured effective values of the vibration speed $v_{(*)RMS(50)}$ [mm·s^{-1}] in the "x", "y" and "z" axes of the selected coordinate system at circumferential speed v_r = 2.5 m·s^{-1} for a conveyor roller with a steel casing of 133 mm diameter. Vibration sensors have been placed at measuring points C and D.

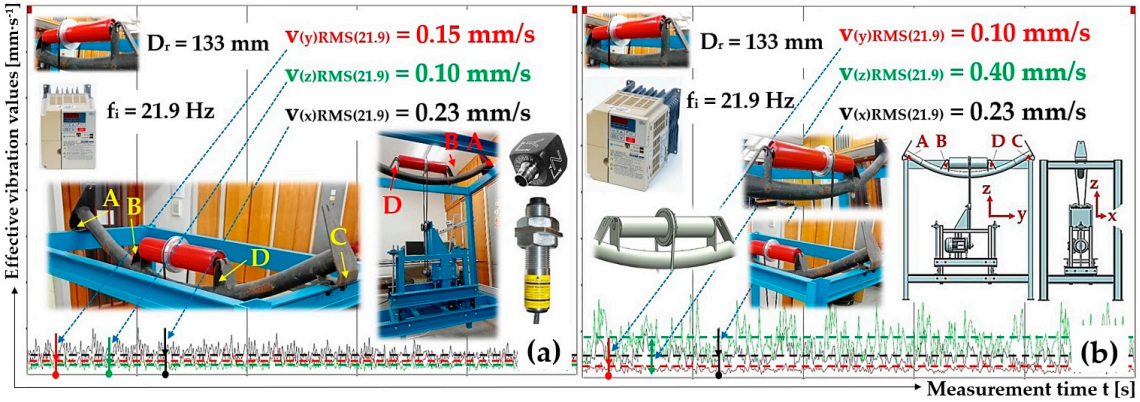

Figure 35. Effective vibration values $v_{(*)RMS(fi)}$ [mm·s^{-1}], steel roller ϕ133 mm, the circumferential speed of the roller v_r = 2.5 m·s^{-1}, steel trestle, **(a)** measuring point C, **(b)** measuring point D.

4. Discussion

The aim of this paper was to detect vibrations transmitted by the rotating casing of the conveyor roller to the fixed conveyor idler and also to the steel frame of the laboratory machine to which the fixed conveyor idler is attached. The measurement of the vibrations of the roller casing installed on a laboratory stand, and an assessment of the technical condition of the belt conveyor rollers after the specified operating time, were also carried out in [33]. In the conclusions of the vibrations measurement of the conveyor roller done by both laboratory machines similar results were achieved.

From the measured time curves of the vibration value (see Figure 12 to Figure 35) for conveyor rollers of 89 mm, 108 mm and 133 mm diameters rotating at circumferential speeds 1.25, 2.5 and 3.85 m·s^{-1}, with the help of the DEWESoft X software, the effective values for vibration velocities were determined, and these are listed in Table 3 to Table 26.

The vibration values of the conveyor rollers show that the effective values of the vibration velocity increase with the increasing speed (circumferential speed) of the conveyor roller casings. This assumption is confirmed in the findings presented in the article [9] by Klimenda et al., who deal in their article [11] with the measurement of the noise and vibration of rollers designed for belt

Preprints (www.preprints.org) | NOT PEER-REVIEWED | Posted: 22 November 2023 doi:10.20944/preprints202311.1342.v1

conveyors. The three highest acceleration values depending on the frequency of the vibration in each direction (*x, y, z)* correspond to the measured effective vibration values $v_{(*)RMS(fi)}$ [mm·s^{-1}] in coordinate axes *(x, y, z). For more information, see Chapters 3.1 to 3.4.*

Figure 36(c) and Figure 36(d) show that the highest effective values of the vibration velocity $v_{(*)RMS(fi)}$ [mm·s^{-1}] reach the conveyor roller with ϕ89 mm diameter placed in the steel trestle of a fixed conveyor idler, and that is in the "z" axis (vertical direction). This fact can be traced in the article [12], in which the three highest values of acceleration depending on the frequency of vibration in each direction are described.

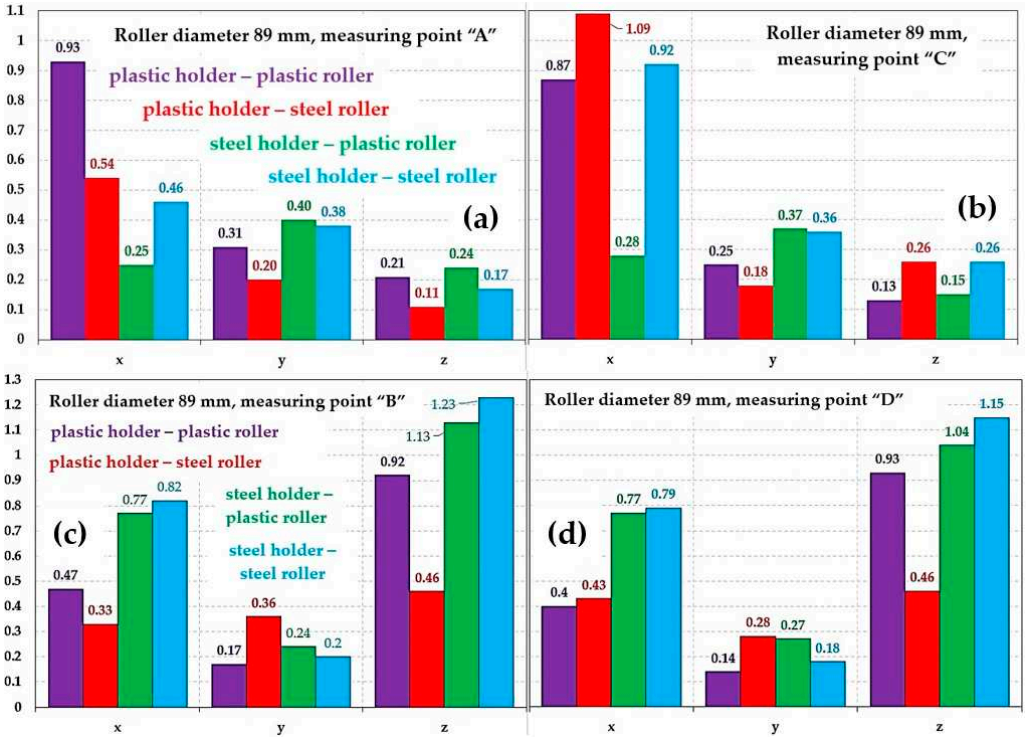

Figure 36. The effective vibration values $v_{(*)RMS(fi)}$ [mm·s^{-1}] of conveyor rollers with a 89 mm diameter, at revolutions 825 min^{-1}. Measuring point as in Figure 11 (a) A, (b) C, (c) B, (d) D.

At the revolutions of the steel casing conveyor roller n_r = 825 mim^{-1} and the roller axle placement of the conveyor with a 89 mm diameter into plastic brackets (see Figure 11 part B), the effective value of the vibration velocity is $v_{(*)RMS(fi)}$ [mm·s^{-1}] in axis "z" is reaching 37.4 % of the value $v_{(*)RMS(fi)}$ [mm·s^{-1}], compared to placing this roller in a steel trestle.

When the axle of the steel conveyor roller ϕ89 mm is fitted into the plastic brackets (see Figure 11 part D), the effective value of the vibration velocity $v_{(*)RMS(fi)}$ [mm·s^{-1}] in the "z" axis reaches 40 % of value $v_{(*)RMS(fi)}$ [mm·s^{-1}], unlike when placed in a steel trestle.

Figure 37c,d show that the highest effective values of the vibration velocity $v_{(*)RMS(fi)}$ [mm·s^{-1}] reach the conveyor roller with ϕ108 mm diameter placed in the steel trestle of a fixed conveyor idler, and that is in the "z" axis (vertical direction).

Preprints (www.preprints.org) | NOT PEER-REVIEWED | Posted: 22 November 2023 doi:10.20944/preprints202311.1342.v1

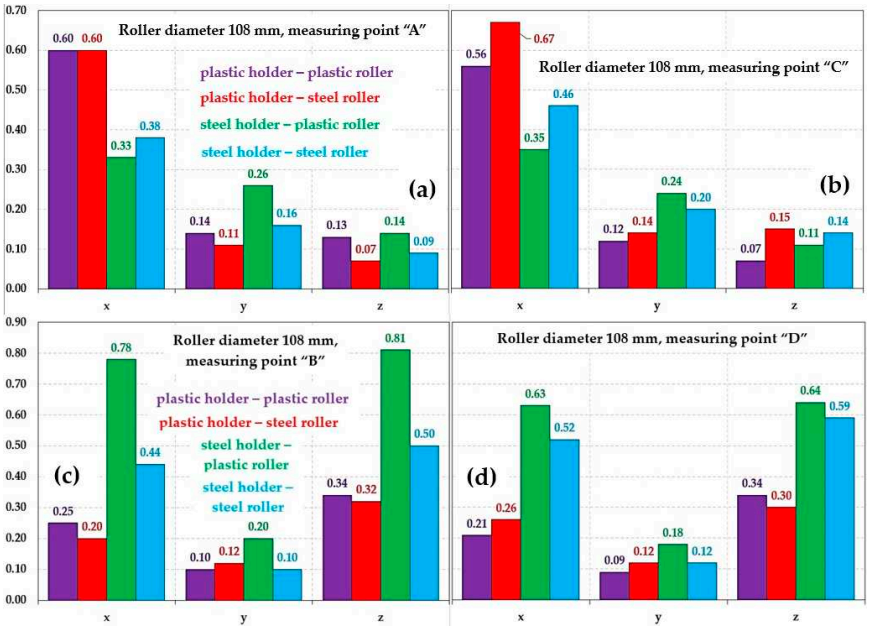

Figure 37. The effective vibration values $v_{(*)RMS(fi)}$ [mm·s^{-1}] of conveyor rollers with a 108 mm diameter, at revolutions 442 min^{-1}. Measuring point as in Figure 11 (a) A, (b) C, (c) B, (d) D.

At the revolutions of the steel casing conveyor roller n_r = 442 mim^{-1} and the roller axle placement of the conveyor with a 108 mm diameter into plastic brackets (see Figure 11 part B), the effective value of the vibration velocity is $v_{(*)RMS(fi)}$ [mm·s^{-1}] in axis "z" is reaching 41.9 % of the value $v_{(*)RMS(fi)}$ [mm·s^{-1}], compared to placing this roller in a steel trestle.

When the axle of the steel conveyor roller ϕ108 mm is fitted into the plastic brackets (see Figure 11 part D), the effective value of the vibration velocity $v_{(*)RMS(fi)}$ [mm·s^{-1}] in the "z" axis reaches 46.9 % of value $v_{(*)RMS(fi)}$ [mm·s^{-1}], unlike when placed in a steel trestle.

From Figure 38c,d, it is clear that the biggest differences in the effective values of the vibration velocity $v_{(*)RMS(fi)}$ [mm·s^{-1}] are reached by the conveyor rollers with a 133 mm diameter, when these are placed in the fixed trestle of a conveyor idle, and these are reached in the "z" axis direction (vertical direction).

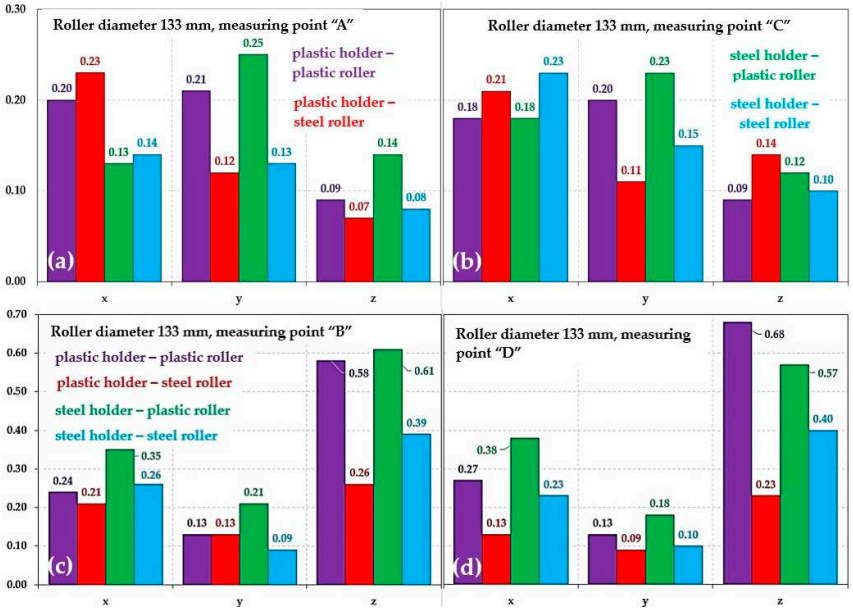

Figure 38. The effective vibration values $v_{(*)RMS(fi)}$ [mm·s^{-1}] of conveyor rollers with a 133 mm diameter, at revolutions 361 min^{-1}. Measuring point as in Figure 11 (a) A, (b) C, (c) B, (d) D.

Preprints (www.preprints.org) | NOT PEER-REVIEWED | Posted: 22 November 2023 doi:10.20944/preprints202311.1342.v1

At the revolutions of the steel casing conveyor roller n_r = 361 mim^{-1} and the roller axle placement of the conveyor with a 108 mm diameter into plastic brackets (see Figure 11 part B), the effective value of the vibration velocity is $v_{(*)RMS(fi)}$ [mm·s^{-1}] in axis "z" is reaching 66.7 % of the value $v_{(*)RMS(fi)}$ [mm·s^{-1}], compared to placing this roller in a steel trestle.

When the axle of the steel conveyor roller ϕ133 mm is fitted into the plastic brackets (see Figure 11 part D), the effective value of the vibration velocity $v_{(*)RMS(fi)}$ [mm·s^{-1}] in the "z" axis reaches 57.5 % of value $v_{(*)RMS(fi)}$ [mm·s^{-1}], unlike when placed in a steel trestle.

In Figure 39, we can see the effective vibration values $v_{(*)RMS(fi)}$ [mm·s^{-1}] for the rotating conveyor rollers measured in the points A to D, of which the plastic or steel casing of a 133 mm diameter rotates at circumferential speed of v_r = 5.74 (3.84, 2.5 or 1.25) m·s^{-1}, provided that the flattened ends of the conveyor roller axles are fitted into the steel or plastic trestle of the fixed conveyor idler.

Graphs (a) to (d) show that the effective vibration values $v_{(*)RMS(fi)}$ [mm·s^{-1}] of the rotating conveyor rollers reach the highest values at higher frequencies set on the frequency converter (the speed of the driving electric motor was controlled by a frequency converter) corresponding to the revolutions of the conveyor rollers.

Research by K. Hicke at al. [53] focuses on monitoring the acoustic condition and detection of roller faults in industrial conveyor belts.

Graphs (a) to (d) also show that higher effective vibration values $v_{(*)RMS(fi)}$ [mm·s^{-1}] that were measured in points A to D, in the case when the axles of the conveyor rollers were placed in a steel trestle (green and blue curves) than when the axles of the conveyor rollers were positioned in plastic brackets (purple and red colour curves).

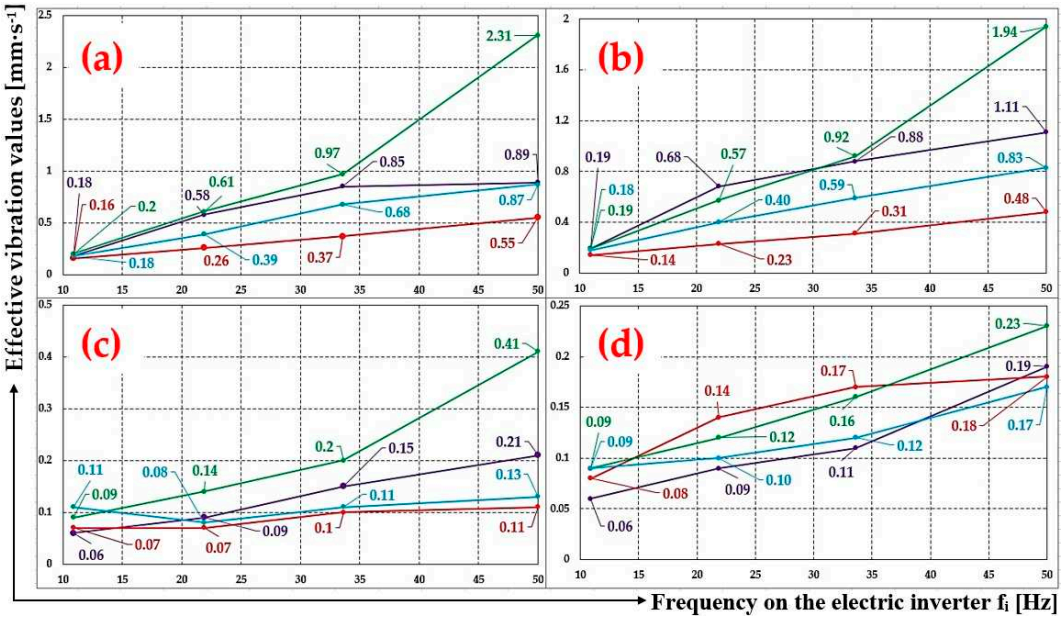

Figure 39. The effective vibration values $v_{(*)RMS(fi)}$ [mm·s^{-1}] of ϕ133 mm conveyor rollers at different revolutions. Measuring point as in Figure 11 (a) B, (b) D, (c) A, (d) C.

In Figure 40, we can see the effective vibration values $v_{(*)RMS(fi)}$ [mm·s^{-1}] for the rotating conveyor rollers measured in the points A to D, of which the plastic or steel casing of a 108 mm diameter rotates at circumferential speed of v_r = 4.66 (3.84, 2.5 or 1.25) m·s^{-1}, provided that the flattened ends of the conveyor roller axles are fitted into the steel or plastic trestle of the fixed conveyor idler.

Preprints (www.preprints.org) | NOT PEER-REVIEWED | Posted: 22 November 2023 doi:10.20944/preprints202311.1342.v1

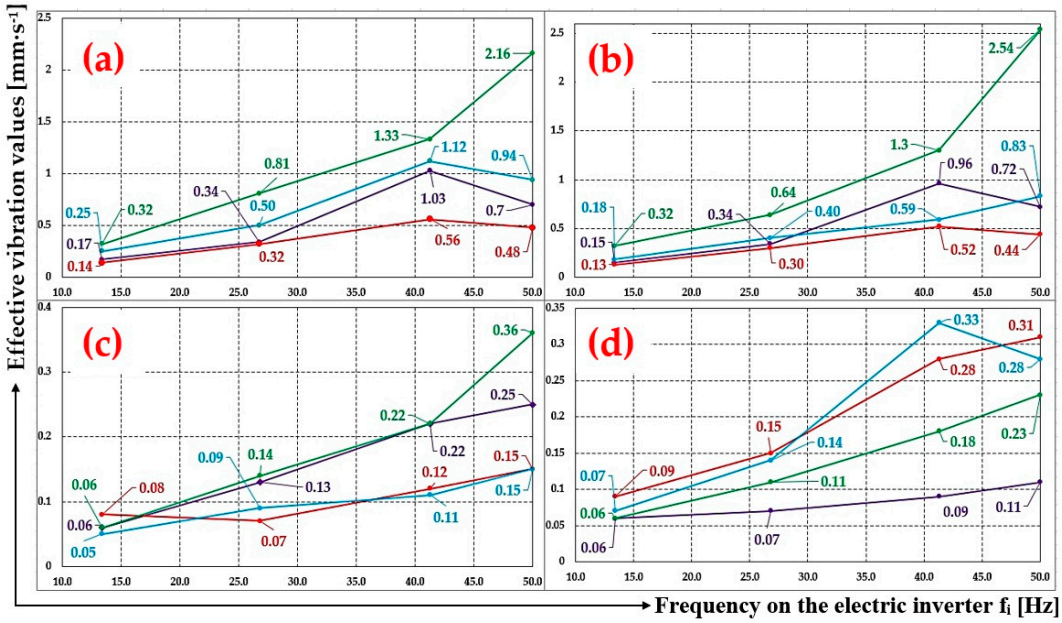

Figure 40. The effective vibration values $v_{(*)RMS(fi)}$ [mm·s^{-1}] of ϕ108 mm conveyor rollers at different revolutions. Measuring point as in Figure 11 (a) B, (b) D, (c) A, (d) C.

In Figure 41, we can see the effective vibration values $v_{(*)RMS(fi)}$ [mm·s^{-1}] for the rotating conveyor rollers measured in the points A to D, of which the plastic or steel casing of a 89 mm diameter rotates at circumferential speed of v_r = 3.84 (2.5 or 1.25) m·s^{-1}, provided that the flattened ends of the conveyor roller axles are fitted into the steel or plastic trestle of the fixed conveyor idler.

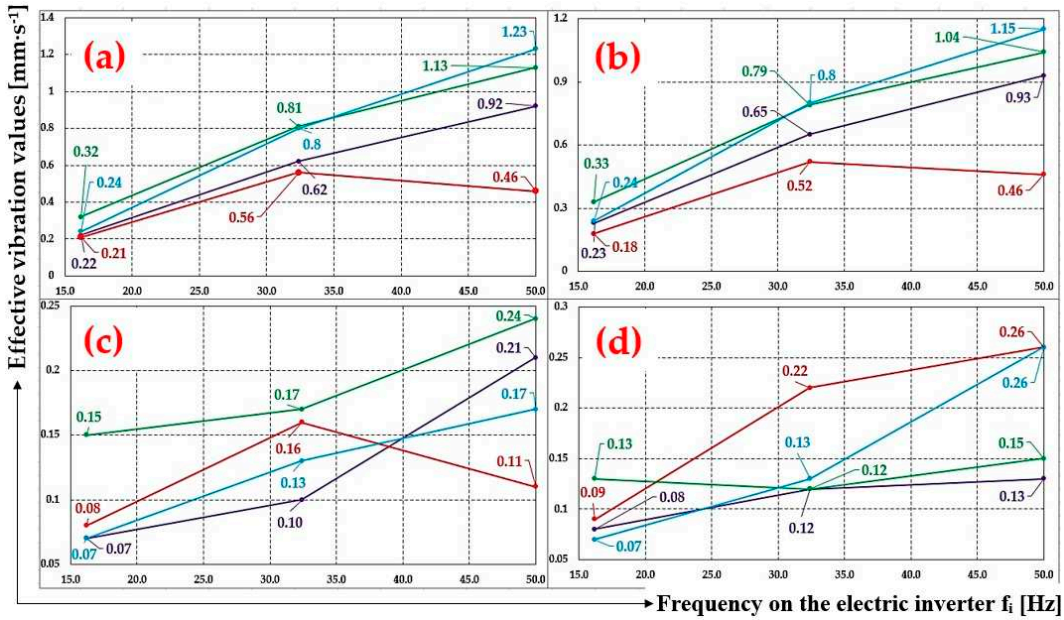

Figure 41. The effective vibration values $v_{(*)RMS(fi)}$ [mm·s^{-1}] of ϕ89 mm conveyor rollers at different revolutions. Measuring point as in Figure 11 (a) B, (b) D, (c) A, (d) C.

The provided vibration measurements of the rotating conveyor rollers with their axles fitted in the steel or plastic trestles of the fixed conveyor idler, performed on the non-rotating parts of our laboratory machine is sufficient to appropriately characterize operating conditions with regard to trouble-free operation. Measurements were made with regard to ISO 10816-1 [6], which specifies the general conditions and procedures for the measurement and evaluation of vibration by means of measurements carried out on non-rotating parts. The general evaluation criteria, which are presented in the form of both magnitude and vibration change, apply to both in-service monitoring and

 doi:10.20944/preprints202311.1342.v1

acceptance tests. The criteria were set primarily with regard to ensuring the reliable, safe and long-term operation of the machine (i.e., a belt conveyor) while minimizing the adverse effects on the connected equipment.

Vibrations lead to fatigue failure or damage which is harmful to engine supporting structures [54].

5. Conclusions

This paper presents a design solution of an experimental machine on which the vibrations of a rotating casing of a conveyor roller can be detected in laboratory conditions. The laboratory machine was created to confirm the theoretical assumption that the magnitude of vibration decreases when the axles of the conveyor roller are placed in plastic brackets. These plastic brackets were attached to the structurally modified trestles of a fixed conveyor idler. This theoretical assumption stated in the article was proved.

The authors of the article carried out experimental measurements based on the measurement of the vibrations of the rotating conveyor roller on the non-rotating parts, i.e., on the trestle of the fixed conveyor idler and in the place of the mechanical attachment of the conveyor idler to the steel frame of the laboratory machine. Vibrations were detected by acceleration sensors, recorded by a measuring apparatus and displayed on a PC monitor in the environment of Dewesoft X software. With the help of software, the measured vibration values were converted into the effective values of the vibration speed, and these were recorded in tables (see Table 3 ÷ Table 26).

The measured instantaneous values of the vibrations at time t [s] were presented in graphs (see Figure 12 ÷ Figure 35). Due to the limited space for the article, in Chapter "3. Results" only the selected measurements records are presented (In case of interest, all records are available from the authors of the article).

The article also describes the design modification of the fixed conveyor idler, the result of which is the installation of plastic brackets in the places where the flattened end parts of the conveyor roller axles are inserted into the notches created in the steel trestle of the traditional fixed conveyor idler. This modified fixed conveyor idler is characterized by two plastic brackets with notches, into which the flattened end parts of the conveyor roller axles are inserted.

The evaluation of the measured data made it possible to conclude that the use of plastic brackets can reduce the vibration values transmitted from the rotating casings of the conveyor rollers into the supporting structure of the belt conveyor. Vibrations generated by the rotating casings of the conveyor rollers in industrial plants with their casings covered with dirt produce excessive secondary noise, which is undesirable in the production hall.

Vibrations and noise are adversely manifested with the higher speed of the conveyor belt, which corresponds directly to the higher revolutions and circumferential speed of the conveyor rollers.

Author Contributions: Conceptualization, L.H. and S.P.; methodology, L.H.; software, S.P.; validation, E.N., T.M. and D.K.; formal analysis, L.H.; investigation, L.H.; resources, D.K.; data curation, E.N.; writing—original draft preparation, L.H.; writing—revie and editing, L.H.; visualization, L.H. and E.N.; supervision, T.M.; project administration, L.H.; funding acquisition, L.H. All authors have read and agreed to the published version of the manuscript.

Funding: This research was funded by "Research and innovation of modern processes and technologies in industrial practice", grant number SP2023/003" and was funded by MŠMT ČR (Ministry of education youth and sports).

Data Availability Statement: Measured data of effective vibration speed values $v_{(*)RMS(fi)}$ [mm·s^{-1}], listed from Table 3 to Table 26 and processed using DEWESoft X software, can be sent in case of interest, by prior written agreement, in *.XLSX (Microsoft Excel) format.

Acknowledgments: In this section, you can acknowledge any support given which is not covered by the author contribution or funding sections. This may include administrative and technical support, or donations in kind (e.g., materials used for experiments).

Conflicts of Interest: The authors declare no conflict of interest. The funders had no role in the design of the study; in the collection, analyses, or interpretation of data; in the writing of the manuscript; or in the decision to publish the results.

References

1. Singiresu, S. R. *Mechanical vibrations*. Boston, MA: Addison Wesley, 1995.
2. Myklestad, N O. *Fundamentals of vibration analysis*. Courier Dover Publications, 2018.
3. Weaver Jr, W., Timoshenko, S. P., & Young, D. H. *Vibration problems in engineering*. John Wiley & Sons, Stanford, California 1991.
4. Bachmann, H. *Vibration problems in structures: practical guidelines*. Springer Science & Business Media, 1995.
5. Buzdugan, G., Mihailescu, E., & Rades, M. *Vibration measurement* (Vol. 8). Springer Science & Business Media, 1986.
6. ČSN ISO 10816-1: Mechanical vibration - Evaluation of machine vibration by measurements on non-rotating parts - Part 1: General guidelines (In Czech: Vibrace - Hodnocení vibrací strojů na základě měření na nerotujících částech -Část 1: Všeobecné směrnice). Available online: https://www.technicke-normy-csn.cz/csn-iso-10816-1-011412-158753.html (accessed on 17 September 2022).
7. Perun, G. Attempt to evaluate the technical condition of the rollers of the belt conveyor by vibration measurements. *Vibroengineering Procedia*, 2014, Volume 3, pp. 296-299.
8. Smith, J. D. *Vibration measurement and analysis*. Butterworth-Heinemann, 2013.
9. Hrabovsky, L.; Pravda, S.; Sebesta, R.; Novakova, E.; Kurac, D. (2023). Detection of a Rotating Conveyor Roller Casing Vibrations on a Laboratory Machine. *Symmetry*, 2023, Volume 15(9), 1626.
10. Peruń, G.; Opasiak, T. Assessment of technical state of the belt conveyor rollers with use vibroacoustics methods-preliminary studies. *Diagnostyka* 2016, Volume 17(1), pp. 75-80.
11. Klimenda, F.; Kampo, J.; Hejma, P. Vibration measurement of conveyor. *Manufacturing Technology* 2019, Volume 19(4), pp. 604-608.
12. Svoboda, M.; Klimenda, F.; Kampo, J.; Soukup, J. Rollers vibration of conveyor belt. *Control and Stability*, Volume 571.
13. Bortnowski, P.; Krol, R.; Ozdoba, M. Roller damage detection method based on the measurement of transverse vibrations of the conveyor belt. *Eksploatacja i Niezawodność*, 2022, Volume 24(3).
14. Peng, C.; Li, Z.; Yang, M.; Fei, M.; Wang, Y. An audio-based intelligent fault diagnosis method for belt conveyor rollers in sand carrier. *Control Engineering Practic*, 2020, Volume 105, 104650.
15. Svoboda, M.; LeComte, D.; Hayes, M.; Heim, R.; Gleason, K.; Angel, J.; Stephens, S. The drought monitor. *Bulletin of the American Meteorological Society* 2002, Volume 83(8), pp. 1181-1190.
16. Zhang, S.; Xia, X. A new energy calculation model of belt conveyor. *AFRICON* 2009, pp. 1-6. **DOI:** 10.1109/AFRCON.2009.5308257.
17. Alspaugh, M. Bulk material handling by conveyor belt III. United States, 2000. https://www.osti.gov/etdeweb/biblio/20242523.
18. Havey, C. R. Belt conveyors for bulk materials. United States 1979. https://www.osti.gov/biblio/6407550.
19. Nascimento, R.; Carvalho, R.; Delabrida, S.; Bianchi, A. G.; Oliveira, R. A. R.; Garcia, L. G. U. An integrated inspection system for belt conveyor rollers. *Proc. 19th Int. Conf. Enterprise Inf. Sys.(ICEIS)* 2017, Volume 2, pp. 190-200.
20. Hou, Y. F.; Meng, Q. R. Dynamic characteristics of conveyor belts. *Journal of China University of Mining and Technology* 2008, Volume 18(4), pp. 629-633.
21. Lozier, M. S. Deconstructing the conveyor belt. *Science* 2010, Volume328(5985), pp. 1507-1511.
22. Hrabovsky, L.; Nenicka, P.; Fries, J. Laboratory Machine Verification of Force Transmission Provided by Friction Acting on the Drive Drum of a Conveyor Belt. *Machines* 2023, Volume*11*, 544.
23. Stace, L. R.; Yardleym E. D. Belt conveying of minerals. United Kingdom: N.p., 2008. https://www.osti.gov/etdeweb/biblio/21036867.
24. Fiset, M.; Dussault, D. Laboratory simulation of the wear process of belt conveyor rollers. *Wear* 1993, Volume 162, pp. 1012-1015.
25. Hrabovsky, L.; Ucen, O.; Kudrna, L.; Cepica, D.; Frydrysek, K. Laboratory Device Detecting Tensile Forces in the Rope and Coefficient of Friction in the Rope Sheave Groove. *Machines* 2022, Volume 10, 590.
26. Folta, Z.; Camlík, P. The conveyor rollers innovation and validation. *Transactions of the VŠB—Technical University of Ostrava, Mechanical Series* 2009, Volume 1(LV), 1651.
27. Hrabovsky, L.; Gaszek, J.; Kovar, L.; Fries, J. A Laboratory Device Designed to Detect and Measure the Resistance Force of a Diagonal Conveyor Belt Plough. *Sensors* 2023, Volume 23(6), 3137.
28. Primary Belt Scraper. Available online: https://www.asgco.com/products/product_category/manufactured-products/conveyor-belt-cleaners/ (accessed on 2 May 2022).

29. Secondary Belt Scraper. Available online: https://www.asgco.com/products/product_category/manufactured-products/conveyor-belt-cleaners/ (accessed on 9 December 2022).
30. Rotary Brush Belt Cleaner. Available online: https://www.alibaba.com/showroom/rotary-brush-belt-cleaner.html (accessed on 20 January 2023).
31. Eliasson, J.; Kyusakov, R.; Martinsson, P. E. (2013). An Internet of Things approach for intelligent monitoring of conveyor belt rollers. In *International Conference on Condition Monitoring and Machinery Failure Prevention Technologies: 18/06/2013-20/06/2013* (Vol. 2, pp. 1096-1104).
32. Malakhov, V.; Dyachenko, V. (2022). Rolling resistance coefficient of belt conveyor rollers as function of operating conditions in mines. *EURASIAN MINING* 2022, Volume. 1. pp. 67–71
33. Alharbi, F.; Luo, S.; Zhang, H.; Shaukat, K.; Yang, G.; Wheeler, C. A.; Chen, Z. A brief review of acoustic and vibration signal-based fault detection for belt conveyor idlers using machine learning models. *Sensors*, 2023, Volume 23(4), 1902.
34. Liu, X.; Pang, Y.; Lodewijks, G.; He, D. (2018). Experimental research on condition monitoring of belt conveyor idlers. *Measurement*, 2018, Volume 127, pp. 277-282.
35. Soares, J. L.; Costa, T. B.; Moura, L. S.; Sousa, W. S.; Mesquita, A. L.; Mesquita, D. S. Machine Learning Based Fault Detection on Belt Conveyor Idlers. In *DINAME 2023 - Proceedings of the XIX International Symposium on Dynamic Problems of Mechanics*, Brazil, February 26 th to March 3rd 2023.
36. Gondek, H; Kolman, J.; Bohac, D. Results of belt conveyors noise reduction with the new construction of roller holders. *International Multidisciplinary Scientific GeoConference: SGEM* 2022, Volume 22(1.1), pp. 369-376.
37. Kolman, J., Bohac, D. Noise reduction of belt conveyor tracks. *International Multidisciplinary Scientific GeoConference: SGEM* 2020, Volume 20(1.2), pp. 195-202.
38. Kulinowski, P.; Kasza, P.; Zarzycki, J. Influence of design parameters of idler bearing units on the energy consumption of a belt conveyor. *Sustainability* 2021, Volume 13, 437.
39. Krol, R.; Kisielewski, W. Research of loading carrying idlers used in belt conveyor-practical applications. *Diagnostyka* 2014, Volume 15, pp. 67–74.
40. Gładysiewicz, L.; Konieczna-Fuławka, M. Influence of idler set load distribution on belt rolling resistance. *Arch. Min. Sci.* 2019, Volume 64, pp. 251–259.
41. Gładysiewicz, L.; Krol, R.; Kisielewski, W. Measurements of loads on belt conveyor idlers operated in real conditions. *Meas. J. Int. Meas. Confed.* 2019, Volume 134, pp. 336–344.
42. Klínový řemen typ SPZ 2500 Lw 9.7x2513 La L=L. Available online: https://www.prumex.cz/klinovy-remen-spz-2500-lw-9-7x2513-la-l-l-profiplus-rubena/ (accessed on 11 July 2023).
43. Třífázový elektromotor 1.5 kW, 1400 RPM. Available online: https://elektromotory-vybo.cz/obchod/elektromotor-1-5kw-1400ot-90l-4-elektricky-motor/ (accessed on 24 January 2023).
44. Ball bearings 6204 2RS. Available online: https://www.fersa.com/en/technical-details/6204%202RS (accessed on 29 April 2022).
45. Vasic, M.; Stojanovic, B.; Blagojevic, M. Failure analysis of idler roller bearings in belt conveyors. *Engineering Failure Analysis*, 2020, Volume 117, 104898.
46. Hand-Arm Acceleration Sensor KS903.10. Available online: https://www.pce-instruments.com/eu/pce-instruments-hand-arm-acceleration-sensor-ks903.10-det_5966162.htm (accessed on 26 September 2021).
47. Sirius Modular Data Acquisition (DAQ) system. Available online: https://dewesoft.com/products/sirius (accessed on 16 February 2023).
48. DeweSoft general catalog. Available online: 1667943193-dewesoft-product-catalog-en.pdf (datocms-assets.com) (accessed on 29 January 2023).
49. ISO 10816-3: Mechanical vibration—Evaluation of machine vibration by measurements on non-rotating parts—Part 3: Industrial machines with nominal power above 15 kW and nominal speeds between 120 r/min and 15 000 r/min when measured in situ (In Czech: Vibrace—Hodnocení vibrací strojů na základě měření na nerotujících částech—Část 3: Průmyslové stroje se jmenovitým výkonem nad 15 kW a jmenovitými otáčkami mezi 120 1/min a 15 000 1/min při měření in situ). Available online: https://www.technicke-normy-csn.cz/csn-iso-10816-3-011412-158763.html (accessed on 28 June 2023).
50. ROLS / ROLS24 Remote Optical Laser Sensor, Instruction Manual. Available online: https://monarchserver.com/Files/pdf/1071-4851-118_ROLS_ROLS24_Manual.pdf (accessed on 26 September 2021).
51. DS-TACHO-3 Technical reference manual. Available online: https://downloads.dewesoft.com/manuals/dewesoft-ds-tacho3-manual-en.pdf (accessed on 14 March 2022).
52. ČSN ISO 1537: Continuous mechanical handling equipment for loose bulk materials. Troughed belt conveyors (other than portable conveyors). Idlers. (In Czech: Zařízení pro plynulou dopravu sypkých hmot. Pásové dopravníky s korýtkovým dopravním profilem (jiné než přenosné). Válečky) Available

online: https://www.normservis.cz/download/view/csn/26/28648/28648_nahled.pdf (accessed on 13 November 2023).
53. Hicke, K.; Hussels, M. T.; Eisermann, R.; Chruscicki, S.; Krebber, K. Distributed Fibre Optic Acoustic and Vibration Sensors for Industrial Monitoring Applications. In *Proceedings AMA Conferences 2017 with SENSOR and IRS2* 2017, pp. 274-279.
54. Ahirrao, N. S.; Bhosle, S. P.; Nehete, D. V. Dynamics and vibration measurements in engines. *Procedia Manufacturing*, 2018, Volume 20, pp. 434-439.